R-8298

LIQUID ROCKET PERFORMANCE COMPUTER MODEL WITH DISTRIBUTED ENERGY RELEASE

INTERIM FINAL REPORT

Contract NAS7-746

by

L. P. Combs
W. D. Chadwick
D. T. Campbell

ROCKETDYNE
A DIVISION OF NORTH AMERICAN ROCKWELL CORPORATION

R-8298

LIQUID ROCKET PERFORMANCE COMPUTER MODEL WITH DISTRIBUTED ENERGY RELEASE

INTERIM FINAL REPORT

by

L. P. Combs
W. D. Chadwick
D. T. Campbell

prepared for

NATIONAL AERONAUTICS AND SPACE ADMINISTRATION

11 September 1970

Contract NAS7-746

Technical Management
Jet Propulsion Laboratory
Pasadena, California

Rocketdyne
A Division of North American Rockwell Corporation
6633 Canoga Avenue, Canoga Park, California

FOREWORD

This report was prepared by Rocketdyne, a Division of North American Rockwell Corporation, in accordance with Article II, Paragraph D of Contract No. NAS7-746 with the National Aeronautics and Space Administration. A NASA contractor report (CR) number was not assigned to the report. The contract period of performance was 15 August 1969 to 15 August 1970. The contract was administered for NASA by the Jet Propulsion Laboratory, Pasadena, California, whose Technical Manager was Dr. Raymond Kushida. The Rocketdyne Program Manager was Mr. Spencer Clapp and Dr. David Campbell functioned as the Rocketdyne Project Manager. Mr. J. C. Hyde and Mr. W. H. Moberly served as valuable consultants with respect to the transonic and supersonic flow aspects of the program.

ABSTRACT

An analytical computer program for performing liquid rocket engine performance analyses was developed by modifying and combining existing spray formation and subsonic combustion computer programs with reference JANNAF (ICRPG) computer programs for transonic and supersonic nozzle flow. The new "Distributed Energy Release" (DER) computer program accounts analytically for the combustion energy release losses resulting from imperfect propellant spray mixing and incomplete spray gasification upstream of the nozzle throat. Based on summing propellant spray contributions from individual injection elements of given type, design and position, the first program block calculates bipropellant spray distribution, drop sizes and velocities at points in a collection-plane, which is also an initial-plane for spray combustion analysis. The second program block analyzes the spray burning and combustion product flow from that plane through the nozzle throat, using a multiple axisymmetric stream tube concept. In the nozzle, a spatial pressure distribution is imposed on the flow as calculated by a supporting transonic flow program block. The final program block calculates two-dimensional, axisymmetric kinetic expansion in the nozzle divergent section of stream tube combustion gases, without further spray burning. Residual spray entering this section was simply treated as mass that is lost and degrades both c* and I_s efficiencies.

Program verification was sought by comparing predicted performance with available experimental data. After some manipulation of spray collection plane location, drop size formulas and method of initializing stream tubes, good agreement of c*-efficiencies for FLOX/LPG propellants was obtained. Parameters varied were like-doublet-pair injection element design details, chamber length and contraction ratio, chamber pressure and mixture ratio. Just one of these cases was carried through to complete calculation of I_s; the calculated value was about 2% higher than expected. Possible causes of this discrepancy are discussed.

CONTENTS

INTRODUCTION

Combustion inefficiencies in liquid rocket engines which result from incomplete spray evaporation, imperfect mixing between propellant sprays and their reacting vapors and incomplete chemical reaction of the combustion products within the combustion chamber have been termed "energy release losses". Such losses normally constitute a major portion of the inefficiency in operation of such rocket engines. The current JANNAF reference method for performance analysis (Ref. 1) accounts for energy release losses in an approximate, empirical manner by an arbitrary reduction in value of the initial propellant enthalpy. Thus, actual hot firing test data have been required to establish apparent values for the energy release loss.

This report describes the development of an improved, physically-based analytical approach wherein these losses are accounted for by incorporation of computer programs for bipropellant spray combustion analysis into the performance analysis methodology. Because the spray burning is distributed throughout the combustion chamber, the improved method is said to have (spatially) distributed energy release.

Qualitatively, energy release losses associated with the physical processes of atomization, spray dispersion and mixing may be traced back through the combustor and attributed directly to injector design characteristics. A major objective of this program was establishment of quantitative, calculable links between injector design details and resultant performance losses. Meeting this objective depends upon capabilities for describing and analyzing in detail the nature and behavior of injected sprays, their subsequent vaporization and burning and the gas dynamics of the multicomponent, multiphase, reacting combustion field. Those capabilities had recently been developed for application to analysis of injector/chamber wall compatibility (Ref. 2), as a series of inter-related computer programs, so the approach taken involved, to a large degree, adaption of some of those computer programs to the performance analysis problem. Certain features of those programs

were refined and they were integrated with (1) an existing transonic analysis program and (2) the JANNAF reference method's two-dimensional kinetic program, which provided for analysis of the supersonic nozzle expansion processes. Formulation of the overall distributed energy release performance model (DER) and its initial checkout and verification are described in this interim final report.

The DER computer program has been delivered to the Jet Propulsion Laboratory, together with supporting documentation to guide its usage (Ref. 3). That documentation includes pertinent program descriptions and listings, input data requirements, operating instructions and a complete sample calculation.

COMPUTER MODEL FORMULATION

In formulating an analytical description of liquid rocket engine combustion and flow processes, it is convenient to subdivide the combustor into a series of discrete zones, as shown in Fig. 1 for a typical configuration. Certainly, transition from one zone to the next cannot

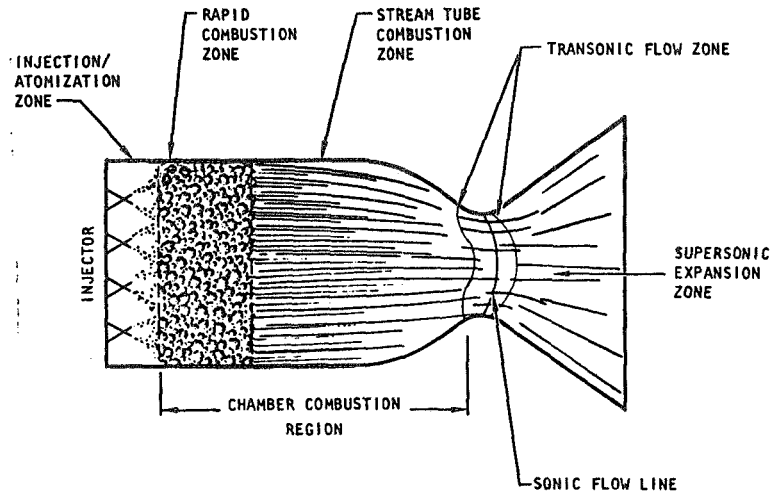

Figure 1. Subdivision of Combustion Chamber into Zones for Analysis

be sharply defined, but is gradual. The positions and abruptness of these transitions are influenced by design variables, propellant combination and operating conditions. A few comments about each of these zones are pertinent before proceeding with description of the computer model.

Immediately adjacent to the propellant injector, the "injection/atomization zone" is least amenable to analytical description. With liquid injection concentrated at discrete sites, large gradients exist in all dimensions with respect to propellant mass fluxes and concentration, degree of atomization and spray dispersion, and properties of the gaseous medium. Spray droplets here are usually cold so the vaporization and burning rates are low. Gases in this zone are primarily either gaseous-injectants or recirculated combustion gases from the next zone downstream.

Completion of primary atomization and convective heating of spray droplets enhance vaporization rates, leading to comparatively high chemical reaction rates in the "rapid combustion zone". Upon burning, the volume of a liquid propellant element is increased 100-fold or more. This expansion forces transverse flows from high-burning-rate sites to low-burning-rate sites as well as producing an axial acceleration. This provides some mixing but the sprays follow the gases only sluggishly, so spray mass flux gradients are primarily degraded by injector-imposed geometric dispersion and interspray mixing[1]. Lateral gas flows will be generated as long as appreciable spray flux gradients persist, but eventually they become small compared with axial flow velocities and the combustion field takes on a stream tube flow appearance.

In the "stream tube combustion zone", the flow lacks the forced transverse convective components that are dominant in the earlier zones. Continued mixing depends upon turbulent exchange between neighboring, parallel-flowing striations, but flow velocities here are high, residence times are short, and turbulent mixing is not very effective. To a good approximation, mixing can be entirely neglected and the two-phase flow treated formally as stream tubes.

As sprays are accelerated and depleted, combustion rate per unit chamber length decays with increasing distance. Chemical reaction rates, on the other hand, remain high well into the exhaust nozzle. Then as the combustion products expand through the nozzle, diminishing pressures and temperatures lower the gas-phase chemical reaction rates. Two-dimensional flow effects are also important in the "transonic" and "supersonic flow" zones. For most high combustion efficiency rockets, spray combustion effects are negligible compared with gas dynamic effects in these downstream zones.

---

[1] The extent and relative importance of the rapid combustion zone depends in large measure on injection element size and spacing across the injector face. With high efficiency injectors (e.g., one having small, closely-spaced impinging elements) this zone may be of rather minimal importance.

Development of an analytical model for the overall combustion process is made feasible only by emphasizing the predominent mechanisms in each of the zones described, allowing processes of secondary importance to be described approximately. For instance, spray vaporization is most important in the subsonic flow regions, where multi-dimensionality and chemical kinetic effects may be simplified or even neglected. Combustion models for much of these regions may be structured quasi-one-dimensionally and emphasize the coupled spray-gas interactions. As another example, burning of residual sprays in the nozzle divergent section may often be neglected, permitting emphasis to be placed on two-dimensional gas dynamics with kinetically-limited reaction rates. These examples will be recognized in the structure of the computer program described below.

COMPUTER MODEL STRUCTURE

A verbal description is given of the overall computer program structure before detailing the formulations for the various combustor zones. Two existing computer programs (both of which were presented and discussed in Ref. 2 and 4) have been modified and interfaced with JANNAF reference computer programs, which have also been modified somewhat. The system of programs has then been linked together to form a single integrated computer program, which is referred to as DER (Distributed Energy Release).

The DER computer program structure is illustrated in Fig. 2. Analysis begins with LISP (Liquid Injector Spray Pattern) computer program calculations of spray mass fluxes, velocity vectors and droplet diameters at a large number of r,θ-mesh points in an "initial-plane" some short distance downstream of the injector face. These calculations are based on injector design data (number and type of injection elements, element locations and orientation) and empirical parameters which

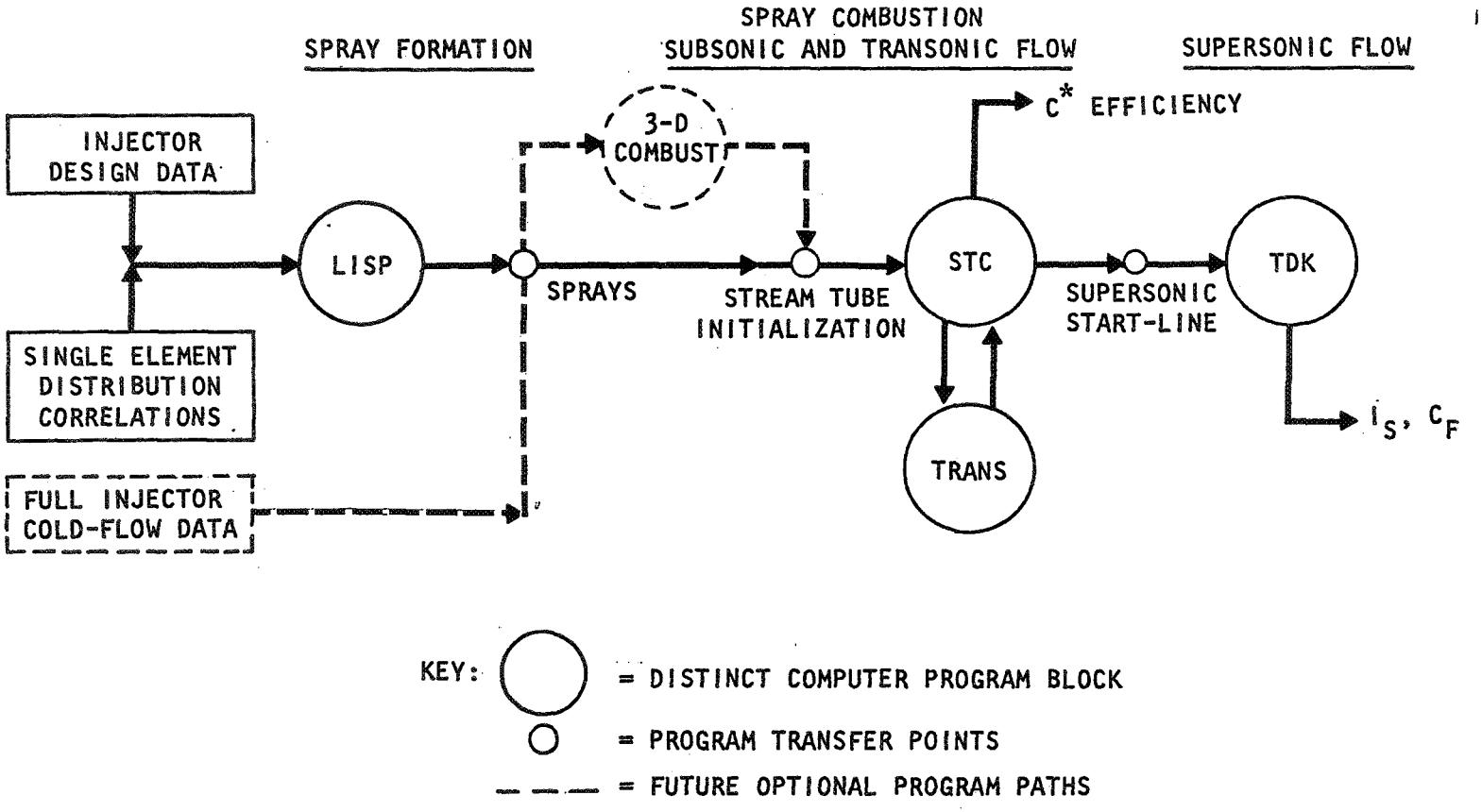

Figure 2. Structure of Distributed Energy Release (DER) Computer Program for Performance Analysis

correlate a single injection element's spray mass flux distribution and mean droplet size with its design and operating parameters. Approximations are also made of propellant vaporization (burning) which occurs upstream of the initial plane.

The output from LISP provides the necessary description of the two-phase flow field for initializing the stream tube combustion program[1]. The assemblage of mesh point flow parameters into stream tubes was done recognizing the eventual necessity of mating with existing ICRPG reference nozzle analysis programs. These ICRPG reference programs describe axisymmetric, two-dimensional flow, i.e., parameters do not vary in the θ-direction of an r, θ, z-cylindrical coordinate system. Therefore, the LISP mesh point flows are combined/averaged in the initial plane to initialize the flows into a number of axisymmetric stream tubes. Typically, there are an order of magnitude fewer stream tubes than mesh points. To avoid excessive degradation of transverse mixture ratio differences, the annular stream tube flows are obtained by a complicated breakdown into a selected number of geometric zones, within each of which the mesh point flows are collected into stream tubes of like mixture ratio.

Spray combustion downstream of the initial plane is analyzed by a stream tube combustion (STC) computer program. Propellant flows (both sprays and gases) which enter a given stream tube are thereafter

---

[1] This approach bypasses analysis of the rapid combustion zone. For injectors with large thrust elements, relatively few elements and/or very non-uniform spray mass distributions, this omission may be seriously detrimental. A three-dimensional combustion computer program (3D-CØMBUST), designed for analyzing this zone, has been developed (Ref. 2). Originally projected to be utilized in the DER program, its omission is discussed briefly on page 9.

constrained to flow in that tube, without exchanges of mass, momentum or energy among neighboring stream tubes. The flow and combustion in each stream tube are analyzed by a one-dimensional formulation, with local stream path as the independent variable. Stream path variations with r-and z-coordinates are accounted for in the nozzle. Solution is obtained by numerical integration, marching in the z-direction from the initial plane through the nozzle throat. The individual stream tubes' solutions in a plane are coupled through constraints on "area continuity" and the radial pressure profile. Pressure is assumed to be constant across each z-plane until, at some point in the nozzle convergent section, curvature due to transonic flow effects is taken into account. Thereafter, rather than continuing to solve for a pressure which satisfies area continuity, absolute pressures are imposed upon the solution. These pressures are calculated by a transonic flow (TRANS) computer program for a nearly equivalent constant flow rate, frozen, homogeneous flow. The sum of the computed flow areas may then deviate from the true geometric flow area. The fractional deviation of the minimum value of that sum from the nozzle throat area then is used to adjust the chamber pressure level for reiteration through all or a portion of the preceding combustion analysis until the throat boundary condition is satisfied.

A supersonic, isobaric start line for the ICRPG Two-Dimensional Kinetic (TDK) computer program (Ref. 5) is then initialized from STC computed data in the neighborhood of the nozzle throat. STC analysis does not provide gas species concentration data, so the equilibrium section of TDK is used to solve for each stream tube's gas phase composition at the TDK start line. The "long-form option" of TDK is used to continue the multiple axisymmetric stream tube analysis through the supersonic expansion process. The subsequent TDK solution is only slightly modified from that given in Ref. 5. Residual unevaporated spray at the initial line is not analyzed further, but is considered to be flow rate that's lost to the gaseous expansion analysis. It is included in the calculation of specific impulse.

Two desirable optional or alternate paths are indicated in Fig. 2 for future inclusion in the DER computer program. The first, direct input of full injector cold-flow data, would be useful for analyzing situations in which single element correlations do not exist but full injector cold-flow data do. The second, provision of three-dimensional combustion (3D-COMBUST) analysis of the early, rapid spray combustion, is expected to be important for analyzing engines with moderately low performance, particularly when there are relatively few injection elements. 3D-COMBUST was originally projected to be utilized in DER. It was omitted from the combined system of computer programs, however, because it had not yet reached a developed, operational status whereby its results could be applied automatically to STC and TDK calculations without prior evaluation of those results by an experienced analyst. Continued improvement and usage of 3D-COMBUST, e.g., Rocketdyne contractual work[1] underway at the time of this writing, should bring the program closer to such a status.

The LISP, STC and TDK computer program blocks have been retained as separate, identifiable entities. Each has been modified somewhat to generate data needed by the following program block and/or to receive data provided by its predecessor. These data are transferred via scratch tapes. Other data required by a program block are read-in via punched cards by that program block. The identity of the TRANS program block has not been so clearly retained. What little input data it needs are read-in by STC and label common blocks are used to transfer data between STC and TRANS.

SUBSONIC COMBUSTION ANALYSIS

Initialization: LISP Computer Program

The LISP computer program is described fully in Ref. 2. Only a brief summarization, condensed from Ref. 4, is given here. The modifications

[1] Contract No. F04611-70-C-0056, "Extension of Injector Chamber Compatibility Analysis," between Rocketdyne and the Air Force Rocket Propulsion Laboratory, Edwards, California, June 1970

to LISP required to fit it into the DER computer program are also indicated.

The LISP computer program calculates spray mass fluxes at mesh points (r, θ, z_o) by the straightforward summation of the mass fluxes from all individual injector elements

$$W(r, \theta, z_o) = \sum_{i=1}^{N_{EL}} w_i (r, \theta, z_o) \qquad (1)$$

which was first applied by Rupe (Ref. 6). The method can be used if: (1) the individual injector elements have predictable spray flux patterns which can be measured and correlated; (2) the individual spray patterns of the various elements are not destroyed, between the element impingement points and the plane z_o, by collisions between neighboring fans; and (3) vaporization of injected spray mass between the element impingement points and plane z_o can be estimated.

The necessary correlation for $w_i(r, \theta, z_o)$ for use in Eq. 1 is based upon the shape of single element spray flux distributions determined from cold-flow spray measurements. Flux patterns were fitted to the generalized expression:

$$w_i(x,y,z) = \frac{w_{001}}{z^2} \left\{ \left[1 + C_1\left(\frac{y}{z}\right) + C_2\left(\frac{y}{z}\right)^2 \right] + \left[C_3\left(\frac{x}{z}\right) + C_4\left(\frac{x}{z}\right)^2 \right] \left[1 + C_5\left(\frac{y}{z}\right) + C_6\left(\frac{y}{z}\right)^2 \right] \right\} e^{-a\left(\frac{x}{z}\right)^2 - b\left(\frac{y}{z}\right)^2} \qquad (2)$$

which is applied separately to each propellant from an element. The (x,y,z) coordinate system in Eq. 2 is referenced to the element's impingement point from which its spray is presumed to emanate. The empirical coefficients a, b, w_{001} and C_1 through C_6 are functions of such parameters as element type (doublet, triplet, etc.) impingement angle, orifice diameter, impinging stream momenta, orifice length, and manifold effects. The coefficients are obtained by correlating data from injector cold-flow simulation tests, in which immiscible propellant simulants are collected in a plane beneath the injector and measured. The form of Eq. 2

was chosen because it satisfies continuity, predicts the observed inverse square relationship between mass flux and distance from the impingement point, and because closed form integrals of Eq. 2 and its x and y moments over the x, y plane allow straightforward evaluation of the empirical coefficients, using experimental cold-flow data.

The LISP computer program transforms the x, y, z coordinate systems of the individual elements to the r, θ, z coordinate system of the thrust chamber and then sums the spray mass fluxes from the individual injector elements to each point in a uniform matrix of mesh points in plane z_o. Droplet velocity vectors are calculated using assumptions that drops travel as straight lines between the impingement point and the mesh points in z_o and that the propellants' injection velocities are conserved by the drops.

Calculation of mean propellant droplet diameters utilizes empirical equations relating them to injection element hole sizes and injection velocities. Since the equations were derived from cold-flow studies with molten wax jets (Ref. 7), corrections accounting for differences in liquid and gas properties between those experiments and the combustor are also applied.

Partial propellant evaporation upstream of z_o is calculated by a simplified, integrated evaporation expression

$$w'(r, \theta, z_o) = w(r, \theta, z_o) \left[1 - \frac{C_{k'} \Delta z}{\bar{D}^2 u_d} \right]^{3/2} \qquad (3)$$

where w' is the liquid spray flux actually arriving at the point (r, θ, z_o). The coefficient $C_{k'}$ is related to the evaporation coefficient k' used in the subsequent spray combustion analysis. However, because the liquid sprays are not fully atomized over the entire Δz distance, values of $C_{k'}$, including a convective Nusselt number, are usually assumed to be only about 1/5 to 1/4 of the stagnant values of k'. The propellant vapors said to be generated by this calculation are summed over all mesh points to yield a single overall vapor flow rate for each propellant. Use of such a simplified evaporation expression is, to some extent, justified by the relatively small percentage of evaporation in the spray formation zone.

Input to the LISP computer program consists of the number, location orientation, size, geometry, and type of injector elements, together with the geometry of combustion zone mesh network and general data concerning the propellant densities and injector pressure drops. Up to 50 injector elements can be considered together with as many as 400 combustion zone mesh points.

For DER utilization the LISP main computer program was converted to a subroutine which generates a scratch tape record of each mesh point's location, reduced spray fluxes, spray droplet diameters and spray velocity vectors and, for the entire chamber segment considered, total and gasified propellant flow rates. The scratch tape is subsequently read by the STC program as a portion of its input data.

Other modifications were made to several subroutines in LISP. Primarily, these dealt with incorporation of more current mean propellant drop size equations for like-doublet and like-doublet-pair injection elements and with spray flux distribution coefficients for like-doublet-pair elements. These are the injector types tested in hot-firing experiments whose results were used for comparative verification analyses, as discussed later.

Axial Marching: STC Computer Program

The STC computer program for multiple-stream-tube bipropellant spray combustion is an extension to axisymmetric flow and transonic nozzle flow of the STRMTB computer program described in Ref. 2 and 4. These extensions complement each other: the assumption that stream tubes are axisymmetric annular cylinders provides positional information which, in turn, makes it possible to impose realistic two-dimensional transonic pressure profiles on the stream tubes. As a result, STC solutions can satisfy quite closely the nozzle boundary condition of gas flux maximization at the throat plane. Additionally, stream tube path length variations can readily be taken into account.

Analytical model solutions are obtained numerically for several systems (one for each stream tube) of simultaneous ordinary differential and algebraic equations by starting with known conditions at the LISP initial-plane and marching downstream in small axial steps.

The degree of satisfaction of throat boundary condition depends upon the consistency of the initial data. A further extension for the STC program was provision for adjustment of initial-plane pressure and reiteration through all or part of the analysis to improve the matching of that boundary condition.

The system of equations for the $i^{\underline{th}}$ stream tube is:

Gas Phase

Continuity:

$$\frac{d}{ds}\left(\rho_i u_i A_{s_i}\right) = A_{s_i} \sum_{n,j} \left(\dot{m}_j^n\right)_i \tag{4}$$

Momentum:

$$\frac{d}{ds}\left(\rho_i u_i^2 A_{s_i}\right) = A_{s_i}\left[-g_c\left(\frac{dp}{ds} + \sum_{j,n} \left(F_j^n\right)_i\right) + \sum_{j,n} \left(\dot{m}_j^n\right)_i \left(u_{dj}^n\right)_i\right] \tag{5}$$

Adiabatic Energy Equation:

$$T_i = T_{oi}\left[1 - \frac{\gamma_i - 1}{2}\left(\frac{u_i}{a_{oi}}\right)^2\right] \tag{6}$$

where

$$T_{oi} = T_o(c_i),\ \gamma_i = \gamma(c_i),\ \text{and}\ M_{wi} = M_w(c_i)$$

are tabulated[1] and

$$a_{oi} = \left[\frac{\gamma_i R_u T_{oi} g_c}{M_{wi}}\right]^{1/2} \tag{7}$$

The local stream tube gas mixture ratio is obtained simply by integrating the evaporation rates to get gasified flowrates:

$$\dot{w}_{ji}(z) = \dot{w}_{ji}(z_o) + \int_{z'=z_o}^{z} \sum_n \left(\dot{m}_j^n\right)_i \, dz' \tag{8}$$

[1]These combustion gas properties are obtained from separate calculation of equilibrium chamber conditions for several mixture ratios and the nominal chamber pressure for a particular case being analyzed. They are also relatively weak functions of chamber pressure, but this dependence is neglected.

Mixture Ratio:

$$c_i = \frac{\dot{w}_{oxid,i}(z)}{\dot{w}_{fuel,i}(z)} \tag{9}$$

State:

$$\rho_i = \frac{p\, M_{wi}}{R_u\, T_i} \tag{10}$$

Spray Phase (n^{th} droplet size group of j^{th} propellant)

Mass Continuity:

$$\frac{d}{ds}\left[(\rho_{dj}{}^n)_i\, (u_{dj}{}^n)_i\, A_{s_i} \right] = - A_{s_i}\, (\dot{m}_j{}^n)_i \tag{11}$$

Drop Number Continuity:

$$\frac{d}{ds}\left[(N_{dj}{}^n)_i\, (u_{dj}{}^n)_i\, A_{s_i} \right] = 0 \tag{12}$$

or, equivalently,

$$(\dot{N}_{dj}{}^n)_i = (N_{dj}{}^n)_i\, (u_{dj}{}^n)_i\, A_{s_i} = \text{constant} \tag{13}$$

Momentum:

$$\frac{d}{ds}\left[(\rho_{dj}{}^n)_i\, (u_{dj}{}^n)_i^{\,2}\, A_{s_i} \right] = A_{s_i}\left[g_c\, (F_j{}^n)_i - (\dot{m}_j{}^n)_i\, (u_{dj}{}^n)_i \right] \tag{14}$$

The independent variable in these one-dimensional flow equations is the stream tube path length or flow direction, s_i. This variable is related to the stream tube's cylindrical (r,z) coordinates through the differential expression

$$ds_i = \left(dz_i^{\,2} + d\bar{r}_i^{\,2} \right)^{1/2} \tag{15}$$

where $\bar{r}_i$ is the stream tube's mean radius. For numerical stability in the STC solution, however, approximations are used that $ds_i = dz$ where the chamber wall is parallel to the axis and that

$$ds_i = dz \left\{ \frac{\left[\bar{r}_i^{\,2} + (z_I - z)^2 \right]^{1/2}}{|z_I - z|} \right\} \tag{16}$$

in the nozzle. The basis for Eq. 16 may be seen by examining Fig. 3.

In this formulation, A_{s_i} appears as a dependent variable for which a solution is to be found. The gas phase equations are constrained, however, in terms of z-plane area:

$$\sum_i A_{z_i}(z) = A_c(z) \tag{17}$$

Therefore, the foregoing equations were modified for the computer program to permit direct solution for A_{z_i} by substituting:

$$A_{s_i} = A_{z_i} \frac{dz}{ds}$$

and neglecting the stream path curvature by saying: $\frac{d^2z}{ds^2} = 0$.

The sets of gas and liquid phase equations are coupled through mass and momentum exchange between phases. For droplet gasification, the simple evaporation coefficient model is utilized:

$$\dot{m}_j^n = N_j^n \left(\frac{\pi}{8}\right) \rho_{\ell_j}^n D_j^n Nu_j^n k'^n_{s_j}$$

where the evaporation coefficient is

$$k'^n_{s_j} = \frac{8}{\rho_{\ell_j}^n} \int_{T_d}^{T} \frac{k_g}{\Delta H_v + \int_{T_d}^{T} c_{p_v} dT} dT \tag{18}$$

and

$$Nu_j^n = 2 + 0.53\, Re_j^n \tag{19}$$

Drag forces on spray droplets are expressed by

$$F_{j_i}^n = \frac{\pi}{8g_c} N_{d_j}^n \rho_i D_j^n C_{D_j}^n \left(u_i - u_{d_j}^n\right) \left| u_i - u_{d_j}^n \right| \tag{20}$$

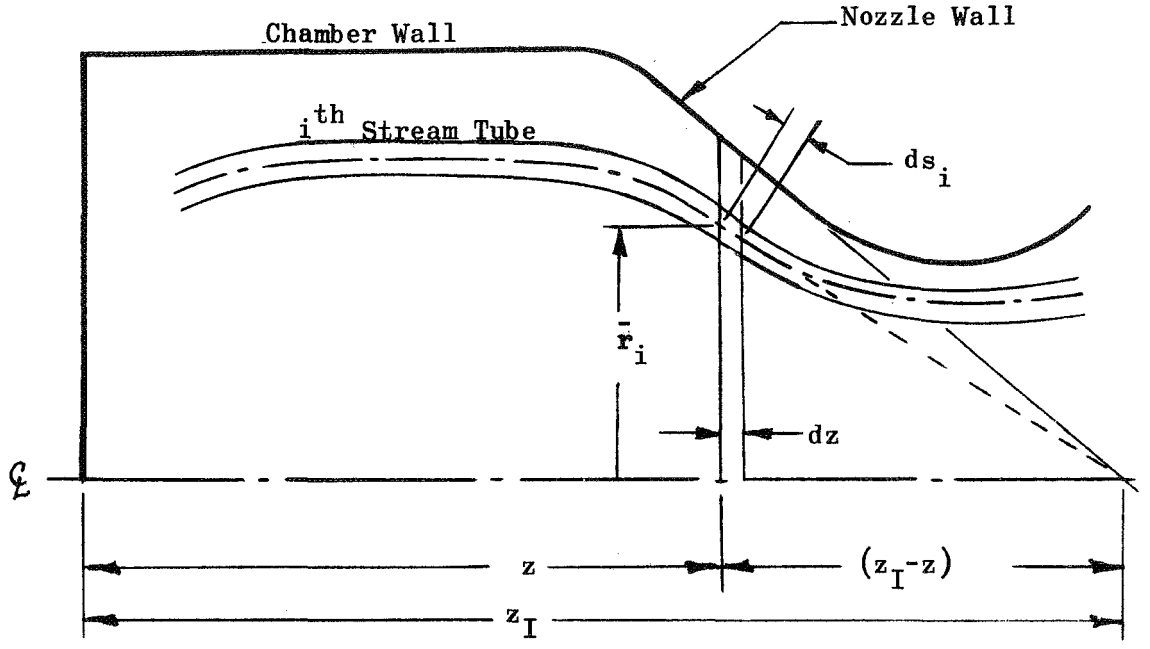

Figure 3. Schematic Illustration of Variables Denoting Local Conical Convergence of Stream Tubes

with the drag coefficient specified as

$$C_{D_j}^{\,n} = 24\,(Re_j^{\,n})^{-0.84} \quad ; \; Re_j^{\,n} \leq 80$$

$$= 0.271\,(Re_j^{\,n})^{0.217} \quad ; \; Re_j^{\,n} > 80 \qquad (21)$$

Input to the STC computer program consists of chamber wall profile, propellant properties, combustion gas properties and either (1) initial-plane gaseous flowrate and mixture ratio and spray flowrates, velocities, and droplet diameters for all spray size-groups entering each stream tube or (2) data from LISP from which these variables can be calculated. Up to 40 stream tubes can be initialized with as many as 12 spray size-groups (fuel and oxidizer combined).

Stream Tube Initialization. Data transferred to STC from LISP are spray mass fluxes, velocities and mean droplet diameters at each (r,θ) mesh point and fuel and oxidizer contributions to total initial-plane gaseous flow rate. In a preliminary version of the program, axisymmetric stream tubes were formed by a straightforward combining of spray flows for all mesh points along each r = constant circle of mesh points into a single stream tube. The initial gas flux was assumed to be uniform and homogeneous. This initialization method was found to introduce a substantial amount of mixture ratio averaging around each annulus when applied to injectors which produce angular gradients in local spray mixture ratio. For some conditions evaluated during program development, combustion efficiencies of 93 to 95 percent were overpredicted by as much as two percent. Thus, more complicated ways were investigated for initializing an order of magnitude fewer stream tubes than initial-plane mesh points without causing excessive mixing.

The method which was ultimately selected provides a non-uniform distribution of gases as well as of sprays. Gas mass fluxes are initially approximated as being uniform at all mesh points and then are adjusted to satisfy species continuity requirements. In the following equations, subscripts i and j correspond to LISP mesh point indices. Uniform gas mass flux is given by:

$$\dot{w}_{g_{ij}} = (\dot{W}_{gF} + \dot{W}_{g0}) \frac{A_{ij}}{\sum_{i,j} A_{ij}} \tag{22}$$

Then the gas mixture ratio at each mesh point is said to be equal to the spray mixture ratio there:

$$c_{ij} = \frac{W_{O_{i,j}}}{W_{F_{ij}}} \tag{23}$$

In general, however, these two assumptions will not be compatible with conservation of propellant species flow rates, e.g.:

$$\dot{W}_{gF} \neq \sum_{ij} \frac{\dot{w}_{g_{ij}}}{1 + c_{ij}} \tag{24}$$

Therefore, the fuel and oxidizer contributions to each mesh point's gas flow are scaled separately to preserve species continuity:

$$\dot{w}_{gF_{ij}} = \frac{\dot{w}_{g_{ij}}}{1 + c_{ij}} \left[\frac{\dot{W}_{gF}}{\sum_{ij} \frac{\dot{w}_{g_{ij}}}{1 + c_{ij}}} \right] \tag{25}$$

$$\dot{w}_{g0_{ij}} = \frac{c_{ij}\dot{w}_{g_{ij}}}{1 + c_{ij}} \left[\frac{\dot{W}_{g0}}{\sum_{ij} \frac{c_{ij}\dot{w}_{g_{ic}}}{1 + c_{ij}}} \right] \tag{26}$$

These definitions complete the specification of propellant flows at each mesh point.

Mesh point flows are combined into stream tubes on bases of both position and local mesh point mixture ratio. First, a chamber wall boundary stream tube is formed by combining the chamber wall mesh points and perhaps one or more circles of mesh points adjacent to the wall on a strictly geometric basis. If the sum of the wall mesh point flows does not exceed 8 percent of the total propellant injection rate, the next inward circle of mesh points is incorporated into the wall

boundary stream tube, etc. This method preserves the angular averaging objected to before, but it is accepted for a fraction of the flow in order to get a wall stream tube that's characteristic of the mean wall mixture ratio.

The remaining circles of mesh points are then subdivided into a few (perhaps 3 to 5) radial zones having roughly equal propellant flow rates. Within each of these zones, the mesh point flows are accumulated according to mixture ratio (rather than position) into several (perhaps 5 to 7) stream tubes with roughly equal flow rates. These stream tubes are then arbitrarily assigned radial positions within the confines of their respective zones. Verification test cases discussed later were analyzed using 19 stream tubes (one at the wall plus six per zone in three radial zones).

Method of Solution. The numerical integration scheme used to solve each stream tube's system of equations is the simplest first-order Runge-Kutta (or Euler) method. Selected for its simplicity, minimal data storage requirements, low execution times and numerical stability, this method's accuracy is strongly dependent upon using sufficiently small step sizes. This limitation is reduced in importance by using backwards differencing in writing finite-difference equations and by solving the equations twice, using predicted values from the first, or predictor, solution as input data for a second, corrector, solution.

The STC program is first run in a single stream tube mode, i.e., a one-dimensional subsonic combustion analysis is made for the entire chamber using appropriate sums and averages of initial stream tube variables. This is done for two reasons: (1) to verify consistency of input data (initial-plane pressure is adjusted until the one-dimensional throat velocity is within a small tolerance of the calculated throat sound speed), and (2) to provide a mean adiabatic expansion coefficient, $\bar{\gamma}$, for combustion gas flow in the convergent part of the exhaust nozzle.

The latter coefficient is given by:

$$\bar{\gamma} = \left(\frac{\ln \frac{\bar{p}^*}{\bar{p}_1}}{\ln \frac{\bar{\rho}^*}{\bar{\rho}_1}} \right) \tag{27}$$

where the subscript 1 refers to the beginning of nozzle convergence, the variables p^* and ρ^* are at sonic flow conditions and the over-bars refer to the one-dimensional flow analysis. It is used by the TRANS computer program (described in the next subsection) to calculate the coordinates of constant pressure surfaces (isobars) for transonic flow in the nozzle. TRANS isobars are generated and transferred to STC in non-dimensional terms, so their use in STC requires knowledge of the nozzle throat radius, R_T (an input parameter), and sonic flow pressure, p^*. Discussion of the evaluation of p^* is included in the following outline of STC's multiple stream tube solution.

Following STC averaged single stream tube analysis and TRANS analysis, the initial plane is reinitialized with its original input and the STC program is run in a multiple stream tube mode. Sequentially:

1. The main iteration loop performs the z direction marching. It begins with estimates that the changes in chamber pressure, stream tube gas velocities and densities across the next Δz increment are equal to their gradients in the preceding single stream tube analysis.
2. These estimated properties are used to calculate predicted values for all spray behavior parameters. Drag, evaporation and other spray droplet size group parameters are computed with controls to: (1) limit evaporation if it is found to exceed the amount of spray available, and (2) avoid having the sign of $\left[u_s - (u_{dj}{}^n)_s \right]_{z_1 \to z_2}$ change in a non-physical way due to overestimation of drag forces, i.e., droplets cannot accelerate or decelerate past the gas velocity within a given Δz.

3. Evaporated sprays are added to the previous gasified propellant sums and the gas phase mixture ratios are computed. Combustion gas properties corresponding to these mixture ratios are obtained by linear interpolation in the properties table. Corrected estimates are then made of gas temperatures, densities, and stream tube areas.

4. Spray gasification and drag terms are next treated as known constants in an implicit-explicit two-step solution for the gas phase properties, stream tube flow areas and chamber pressure in plane z_2. In the first step, a pressure level in plane z_2 is assumed in order to calculate a predicted distribution of stream tube areas in that plane. In the second step, that distribution of areas is assumed to be valid, making possible an explicit solution for the gas temperatures, densities and pressure at z_2.

5. The foregoing paragraphs 2, 3, and 4 describe a predictor cycle. Their calculations are repeated in a corrector cycle, using the predictor cycle's calculated z_2-plane results instead of the estimated properties (paragraph 1). If evaporation of a spray group is calculated in the corrector cycle to exceed the total mass of that group, the group is said to be completely gasified. (For improved accuracy, a user may elect to perform additional corrector cycles.)

6. At this point, normal program flow is printout of computed data at plane z_2, reinitialization of plane z_1 at plane z_2 for a new Δz and progressing again through the paragraph 1 through paragraph 5 computations. This procedure would continue all the way to the nozzle throat for non-axisymmetric stream tubes. With DER's axisymmetric annular stream tubes, however, the procedure is changed at the position in the nozzle where curvature of the isobaric surfaces is introduced.

7. An approximate value of p* is estimated from the nozzle throat plane pressure of the preceding averaged, single stream tube analysis $p^* = \bar{p}^* \, p(z_o)/\bar{p}(z_o)$, where z_o refers to the ITSP collection, STC initialization plane. By multiplying the reduced

pressures, p/p^*, of the TRANS isobars by this value of p^*, absolute pressures are calculated for the transonic flow field. These are imposed upon the multiple stream tube nozzle flow.

The furthest upstream TRANS isobar may be planar or curved, depending upon the nozzle's radius ratio and shape of its convergent section. If it is curved, it is desirable to introduce a gradual transition from planar isobars to that first curved isobar that the solution encounters. Also, a gradual transition is desirable to smooth out any discontinuity in pressure levels between those solved for upstream and imposed downstream of the transition. The gradual transition is provided by stopping the solution for pressure level at a position that is upstream of the nozzle throat by 1.3 times the axial distance that the furthest-upstream TRANS isobar intersects the nozzle wall, and using linear interpolation to impose absolute pressures over the transition interval.

In the transonic region, imposition of absolute pressures makes the paragraph 4 solution for pressure level redundant, so that the gas phase calculation is reduced to a one-step, explicity solution for stream tube areas. Because absolute pressures have been imposed, the solution now provides absolute values of stream tube areas and these may or may not sum to the local nozzle flow area (i.e., satisfy area continuity). By this method, area continuity can be satisfied only by finding the appropriate value of p^* to define the proper nozzle pressure level.

8. As the solution marches through the transonic flow regime, the minimum value of the sum of the calculated stream tube areas at any preceding z-plane is stored. Later, after the solution has reached a z-plane that's wholly downstream of the TRANS isobar which intersects the nozzle wall at the throat (TDK start-line), this minimum area sum is compared with the input geometric area of the nozzle throat. (It is the match of these areas that constitutes satisfaction of the nozzle throat boundary condition.) If the fractional deviation is less than some input tolerance, ϵ_{A_t}, the TDK start-line is initialized. If

the deviation lies between one and three times ϵ_{A_t}, the value of p* is adjusted and the solution is recalculated from the point in the nozzle where absolute pressures were imposed. For deviations exceeding $3\,\epsilon_{A_t}$, the STC initial-plane pressure is adjusted and the entire multiple stream tube solution is recalculated.

Transonic Nozzle Flow: TRANS Computer Program

The reference TDK computer program (Ref. 5) has a transonic flow analysis section which, among other calculations, provides, r,z-coordinates of an isobaric start-line for the supersonic expansion. This section was initially removed from the TDK program and modified so that it generated a family of as many as twenty isobaric lines throughout the transonic flow regime. The necessary input data were supplied from the averaged, single stream tube solution of STC, so this initial TRANS program gave a homogeneous flow solution. Its application was limited, just as it was in TDK, to nozzles whose ratios of throat-radius-of-curvature to throat-opening radius are not smaller than two.

The restriction on nozzle radius ratio subsequently has been relaxed (Ref. 8) by replacing the foregoing transonic flow analysis section of TDK with a new section based on a solution method (Ref. 9) which gives stable solutions for homogeneous flows with radius ratios as small as 5/8. That improved replacement section of TDK was modified to obtain a second version of TRANS for DER program usage. This second version is hereafter referred to as the TRANS computer program.

As input data, TRANS needs values only of the nozzle throat radius, R_R, and a mean expansion coefficient, $\bar{\gamma}$. Isobaric coordinates are calculated in terms of axial distance, X, from the throat plane and radial distance, R, from the nozzle axis; both dimensions are normalized to the throat radius. Multiple isobars are generated, one at a time, by starting downstream of the throat and marching upstream with equal intervals,

$\Delta\alpha$, in the angle between the nozzle axis and a line tangent to the nozzle wall at the isobar/wall intersection point. The program is structured such that that intersection point for the fifth isobar is at the throat; this isobar later becomes the TDK start-line. Four isobar/wall intersection points lie downstream of the throat ($\alpha > 0$) and the remainder lie upstream of the throat ($\alpha < 0$). The angular interval between isobars is given by:

$$\Delta\alpha = -\left(1 + \frac{2}{R_R}\right) \tag{28}$$

Generation of isobars continues until either (1) there are twenty of them or (2) an isobar exhibits significant reverse, or upstream curvature. In the latter case, that last upstream-curving isobar is replaced with a planar surface.

Two computer-plotted examples from TRANS analyses are shown in Fig. 4, where: the nozzle axis is at the bottom (R/RT = 0); flow direction is from left to right; a portion of the nozzle wall, defined by $-30° \leq$ wall angle $\leq +8°$, is shown as the upper curve; isobars are generated from right to left at nozzle wall angle intervals of 2.00° (Eq. was not used in these runs). The monotonic downstream curvature of the constant pressure surfaces is apparent, as is its accentuation by lowering the nozzle radius ratio. Included on the figure are tables which list the pressure ratio, p/p*, and Mach number for each isobar.

Calculation of a nozzle discharge coefficient was added to the TRANS program using the 3rd order equation given in Ref. 9:

$$C_{ND} = 1 - \frac{\bar{\nu}+1}{(1+R_R)^2}\left[\frac{1}{96} - \frac{(8\bar{\nu}-27)}{2304(1+R_R)} + \frac{(754\bar{\nu}^2 - 757\bar{\nu} + 3633)}{276,408(1+R_R)^2}\right] \tag{29}$$

Before proceeding to multiple stream tube STC program analysis, the STC initial-plane pressure which satisfied one-dimensional sonic throat flow is divided by C_{ND} to obtain an improved estimate of initial plane pressure and expedite convergence on the nozzle throat boundary condition.

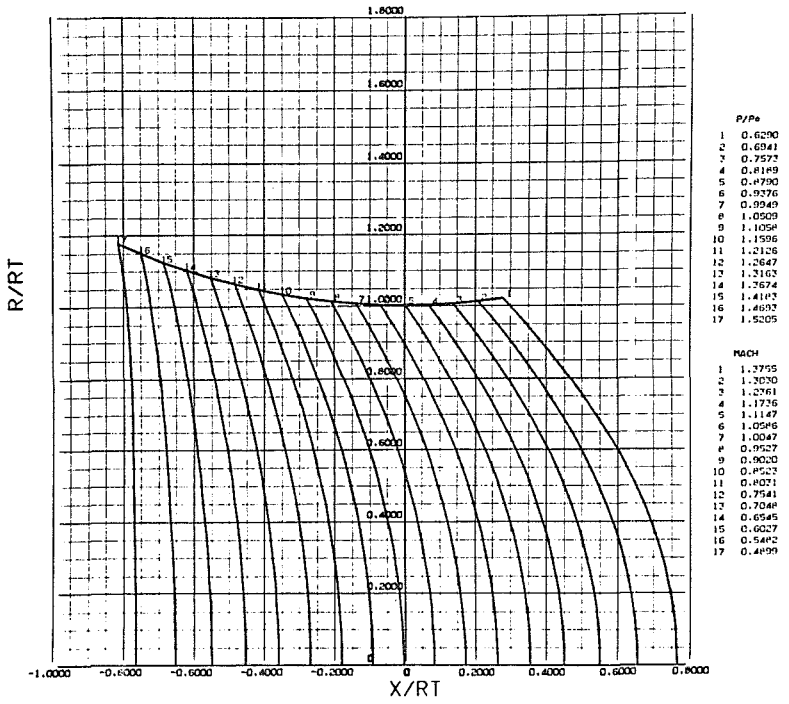

a) Radius Ratio = 2.00

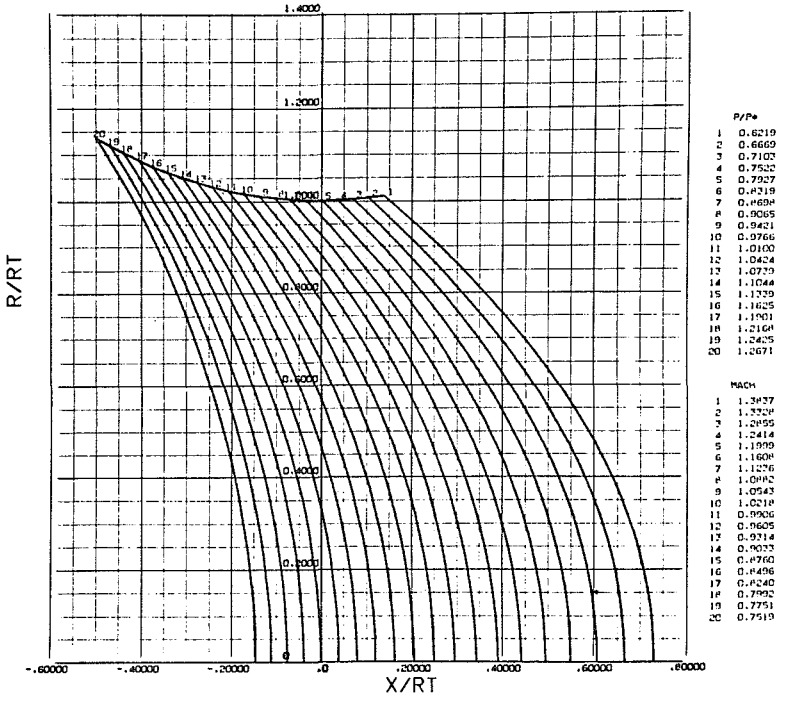

b) Radius Ratio = 1.00

Figure 4. Nozzle Pressure Distributions Calculated by the TRANS Computer Program

SUPERSONIC NOZZLE EXPANSION: TDK COMPUTER PROGRAM

The TDK computer program block of the DER computer program is a shortened and somewhat modified version of the reference TDK program (Ref. 5). The basic approach was to initialize the TDK start-line via data calculated by the STC program, supplementing those data with TDK computations as required, and to retain the multiple axisymmetric stream tube nature of the solution by utilizing TDK's long-form option. To the extent possible, modification of the reference program was held to a minimum.

Initialization from STC Data

Coordinates and flow direction at 40 points along the isobaric TDK initial-line, computed by TRANS, are transferred to TDK. In the STC analysis, the intersections of dividing-stream-lines (between neighboring stream tubes) with the TDK initial-line are found and their coordinates are transferred to TDK. Also transferred to TDK are the gas mixture ratio and velocity at each stream tube's intersection with the initial-line. The initial-line pressure and a mean vaporization efficiency complete the specification of data from STC.

The composition of each stream tube's combustion gases must be specified at the initial line. The simplified tabular specification of stagnation combustion product properties as functions of mixture ratio, whic is used in STC, essentially provides local isentropic frozen expansion. Species concentrations are not included in that specification because they are not needed for STC computations. Therefore, the equilibrium analysis section of TDK is used to obtain equilibrium initial line conditions for each stream tube, based on the specified mixture ratio, flow velocity and pressure. In addition to gas composition, the molecular weight, temperature and density are derived from the equilibrium solution; thus, these flow parameters may be discontinuous at the initial line because of the abrupt change from essentially frozen to equilibrium flow.

TDK Program Modifications

A large part of the reference TDK program is identical to the reference ODK (one-dimensional kinetic) computer program. That section of TDK has been modified for DER program usage by:

1. Solving for equilibrium conditions only at the initial-line point in the flow, rather than at chamber stagnation, throat position and an expansion point (avoids generation of unneeded data).
2. Performing that initial line equilibrium solution repetitively, once for each stream tube.
3. Bypassing the one-dimensional kinetic nozzle flow analysis.

The transonic flow analysis section of the reference TDK program has been replaced completely. Transonic flow is no longer analyzed here; the functions now performed by this section are distribution of 49 discrete initial line points among the stream tubes and assignment of appropriate flow properties to those points. Two points, having identical coordinates but different properties, are required to define a dividing stream line between stream tubes. This limits to 24 the number of stream tubes which can be initialized. If there are n_t stream tubes, there are $49-2\ n_t$ extra points which are assigned as interior points of the widest stream tubes. The foregoing equilibrium flow properties for each stream tube are then assigned to all initial line points associated with it.

The section of TDK which calculates the supersonic, kinetic expansion in the nozzle downstream of the initial-line has been modified to account for the reduction in specific impulse due to incomplete combustion, i.e., unevaporated propellants passing through the nozzle throat. In the reference program, specific impulse is calculated at any given point in the solution by dividing a local integrated value of thrust by the total gaseous flowrate, obtained by integrating ρu over the initial-line. In the modified version, that total gaseous flowrate has been replaced by a total propellant flowrate.

No account is taken of continued evaporation or acceleration that unevaporated propellant sprays might undergo in the supersonic nozzle expansion section. Neither is their momentum added to the initial line impulse; this omission was made consciously, in the belief that it responded to a JANNAF subcommittee discussion concerning the likelihood that the calculated gas-phase momentum would be too high because the residual spray's kinetic energy had not been deducted from the total combustion gas energy. A subsequent order of magnitude analysis has indicated that the kinetic energy effect is small compared to the neglected momentum effect and, therefore, that this omission is invalid and should be corrected.

If condensed species are found to exist at any point along the TDK initial-line, the reference TDK computer program terminates the analysis and does not perform the supersonic expansion calculations. Because one or more stream tubes may be at mixture ratios which produce some condensed combustion products, the DER version of TDK was modified to bypass this termination control. The mass of the condensed species is neglected and the mass fractions of the attendant gaseous species are normalized so that their sum is unity.

COMPUTER PROGRAM OPERATION

The DER computer program was developed for operation on Rocketdyne's IBM System 360, Mod 50/65 computer which is designed to run programs written in Fortran H. So that this program would be compatible with other computers, however, it was written in Fortran IV (which is a subset of Fortran H). There are, of course, some sub-programs which may not be operable on other than the Rocketdyne computer; for most other computers, these are probably restricted to the data-plotting functions and can be replaced by dummy subroutines without detriment to the rest of the program functions. In order to run the program on any computer, a user must supply program control cards that are compatible with his compiler, link editor, etc. The program makes extensive use of overlay in order to reduce computer storage requirements; approximately 50,000 words are needed.

Operation of the DER computer program also depends upon a user-supplied data deck, through which he specifies details for the particular combustor and propellants he desires to analyze. Details concerning the assemblage of a data deck and a complete sample calculation are given in Ref. 3. Brief summarizations of the calculation procedure and program output are given in the following paragraphs.

CALCULATION PROCEDURE

Initially, the calculation procedure for the DER computer program involves expenditure of a substantial effort to assemble a data deck. There are separate sections of the data deck for each of the major program blocks except TRANS; they are assembled in the order in which the program calculations proceed (Fig. 2).

DER main control program input consists only of a set of comment cards describing the case and a set of four flow control integers, whose values determine whether LISP, STC, TRANS and TDK program blocks are utilized.

The LISP computer program block may require a fairly large input data deck, depending upon the complexity of the injector design and upon whether the injection element types used are represented in the LISP library of distribution correlations. A user must study his injector design to determine what, if any, pie-shaped sector of the injector/combustor is truly representative of the entire combustor. An appropriate mesh size is denoted by specifying Δr and $\Delta\theta$. He must then decide how many injection elements supply spray to that sector, whether or not it is desirable to analyze only elements that lie within the sector and, if so, what kind of spray flux symmetry exists at lines of symmetry bounding the sector. He must make certain that the sector gets just its proportionate share of the total injected flows. Each injection element's type, location, orientation, scale (hole diameters), discharge coefficient and propellant species must be given. Additional input of mean drop sizes and mass distribution coefficients are required for element types not represented in the LISP library.

Key adjustable parameters are the evaporation coefficients, which control the approximation of spray combustion upstream of the LISP collection-plane, and the location of the collection-plane, z_o. The value of z_o usually has a significant influence on the degree of propellant mixing achieved by LISP and, therefore, has a direct effect on calculated efficiency. User experience concerning atomization distances, spray spreading rates, etc., can be invaluable in selecting an appropriate z_o but he should also give strong consideration to available peripheral information, e.g., cold-flow characterization of injector flows and the degree of success of previous analyses of related injector designs.

The LISP collection-plane is the STC initialization plane. The combining of LISP mesh point flows into stream tube flows is controlled by specifying the number of geometric zones to be considered and the number of stream tubes in each zone. The user exercises no further control over this process. He can specify that there are only two

propellant spray size groups, one each for the oxidizer and fuel; otherwise, the program will select a total of twelve size groups, six for each propellant.

STC computer program block data deck input are concerned principally with the combustor geometry, combustion gas properties tables, propellant properties and thermodynamic properties used for calculating spray evaporation coefficients. It is important that a reasonable effort be devoted to obtaining best available values or estimates.

The STC-marching interval, Δz, is specified implicitly by stating the number of Δz's between z_o and the nozzle throat. Too small a value of Δz will result in excessive computer times and too large a value will degrade the accuracy of the solution. Values of $0.033 \leq \Delta z \leq 0.10$-inch have been used in DER checkout analyses. Other user options that may influence both accuracy and computer time are the number of corrector cycles made in each Δz step, and the tolerances placed on convergence upon the throat boundary condition. Too tight a tolerance may require an excessive number of iterations through the STC analysis, resulting in excessive execution times. Input variables specify the maximum number of iterations allowed for both the single and multiple stream tube analyses.

There are no user options concerning the operation of the TRANS computer program block or the transfer of data from STC to TDK. The TDK portion of the data deck is quite small compared to those portions for LISP and STC, consisting principally of some propellant thermochemical data, nozzle throat and divergent section geometric data. The user can input data to override a number of default options, such as numbers of iterations, integration stepsize, convergence tolerances, etc. Some of these may influence the performance predictions but they have not been explored with respect to DER program usage.

COMPUTER PROGRAM OUTPUT

Each of the major program blocks of the DER computer program has its own distinct output. Printout is the principal output for each section, and there is some graphical output. Punched card output is also provided to make it possible to reperform STC or TDK analyses for a case that's already been run without having to rerun the program blocks preceding the one(s) which are being rerun. (For example, the same LISP output might be used for several STC and TDK runs with different chamber and nozzle lengths, or TDK might be rurun with different nozzle contours or expansion ratios using a single STC output.)

DER program graphical output is illustrated in Fig. 4 through 7. From the LISP program, two of four types of data plots are reproduced in Fig. 5. LISP analysis considers a specified sector (Fig. 5a) of the full, circular chamber cross-section; for contour plots (Fig. 5b) and corresponding shade plots (not illustrated), the data are expanded to permit plotting the full chamber cross section. Also not illustrated, LISP generates graphs of fuel and oxidizer mass flux around selected r = constant surfaces. The TRANS program graphical plot of nozzle isobars (Fig. 4) has been discussed earlier. From STC analysis, an axial cross-section of a typical cylindrical chamber appears in Fig. 6. Dividing streamlines between stream tubes are plotted, beginning at the STC initial-plane and continuing through the nozzle throat. To illustrate the physical nature of TDK output, Fig. 7 is included here, even though it is not a computer-generated data plot. The reader interested in further output details is referred to Ref. 3.

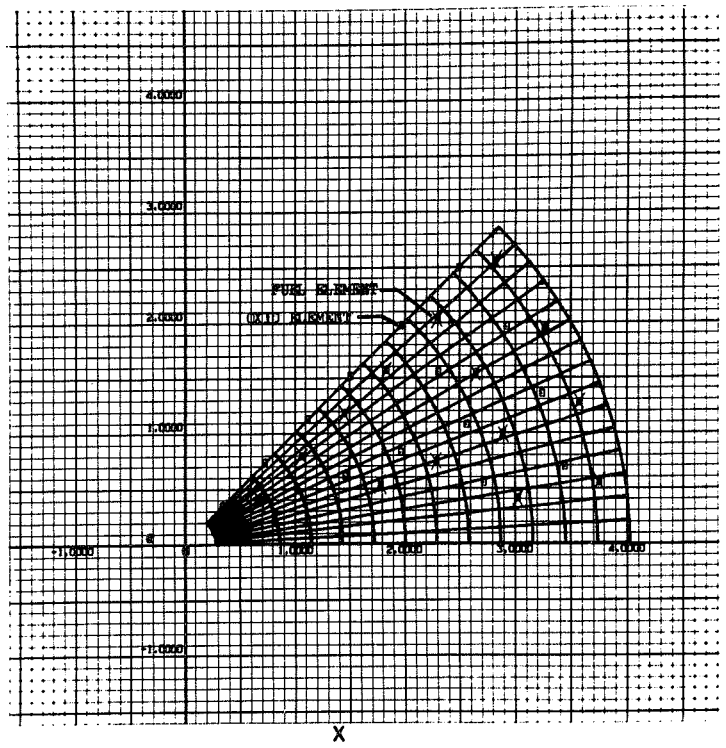

a) Injector Segment, Showing Mesh System and Element Locations

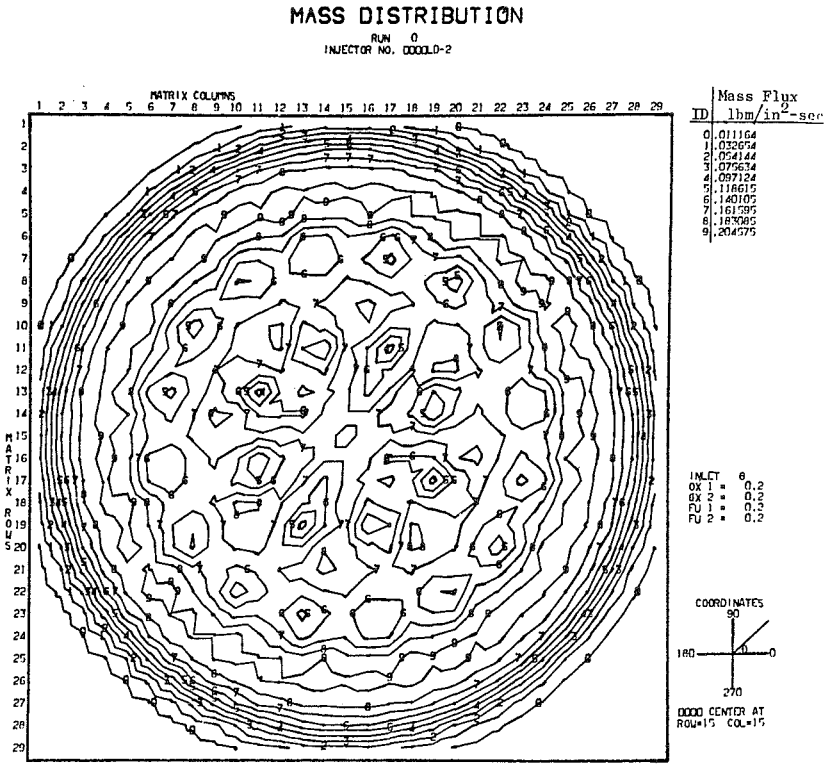

b) Full Injector Contour - Plot of Mass Flux Distribution

Figure 5. Examples of Computer-Plotted Data from LISP Program Block

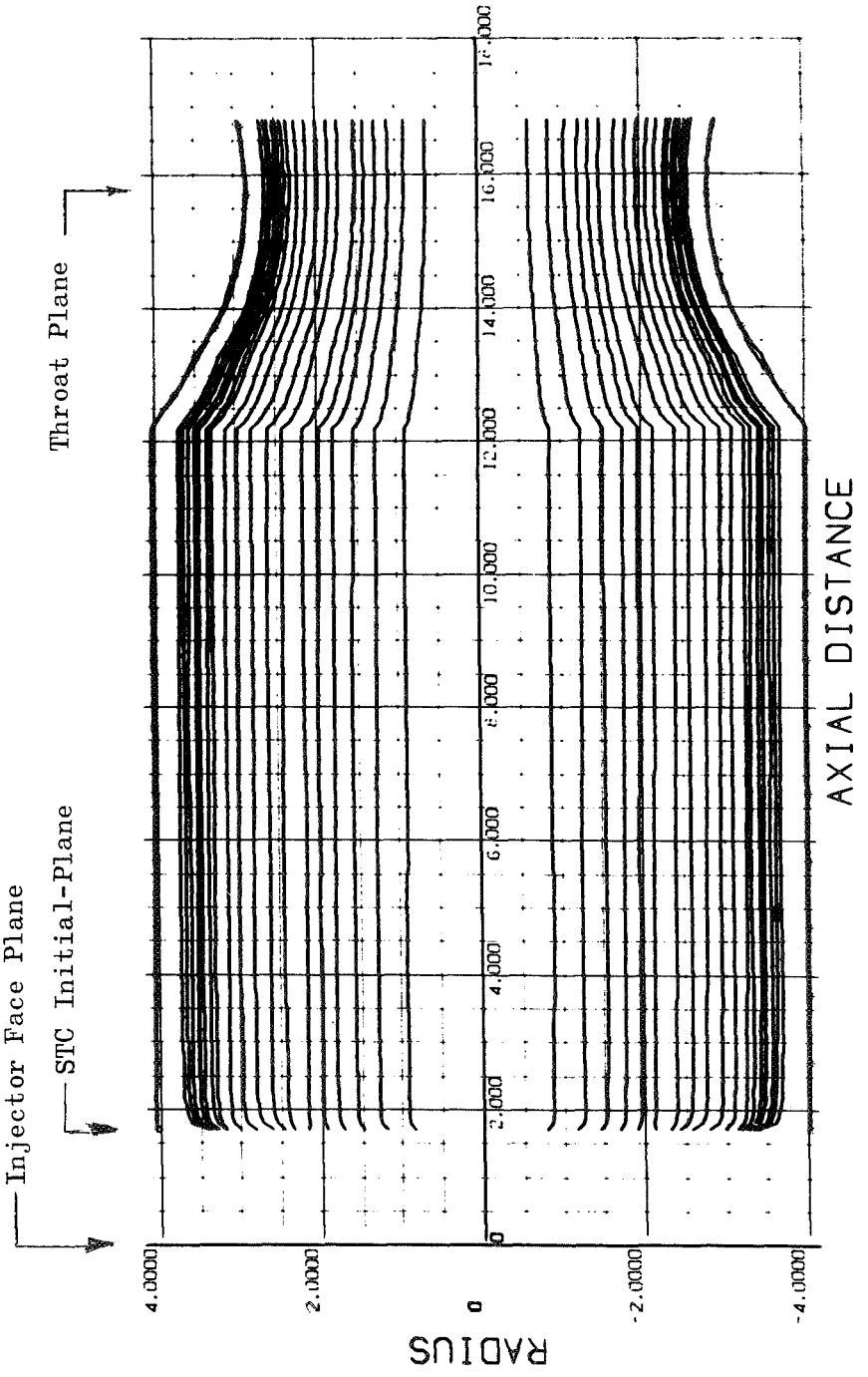

Figure 6. Example of Computer-Plotted Dividing Stream Lines from STC Program Block

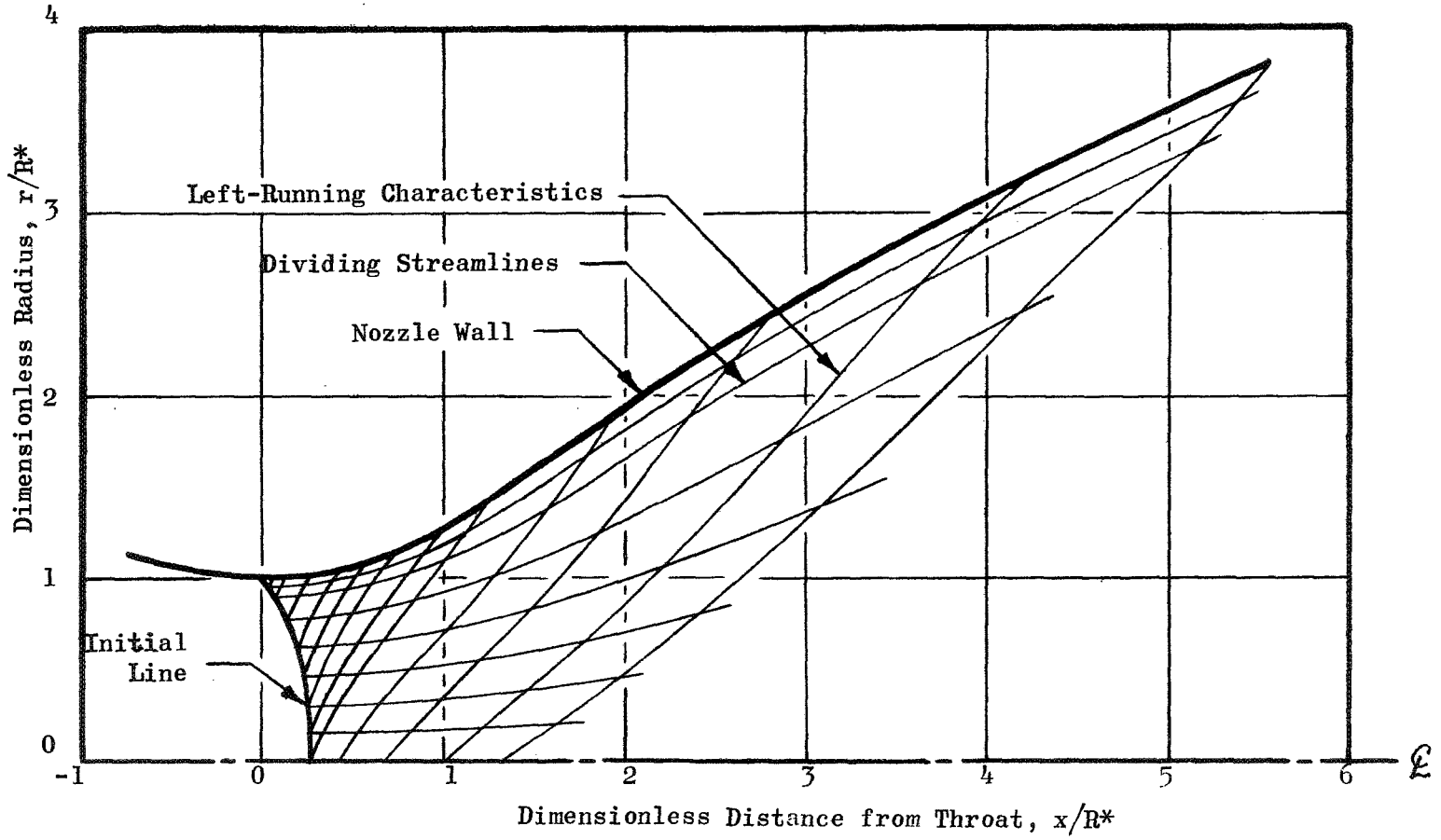

Figure 7. Manually-Plotted Coordinates of Dividing-Stream-Lines and Left-Running-Characteristics from TDK Program Block

VERIFICATION OF MODEL VALIDITY

NOMINAL CHECKOUT CASE

The DER computer program was developed and checked out using a single set of input data corresponding to a particular available set of design and operating conditions of an engine which previously has been hot-fired. Details follow for this nominal checkout case, which was selected from several described in Ref. 10 for FLOX (80% F_2-20% O_2)/LPG (55% CH_4-45% C_2H_6). An 8.06-in diameter, 30-in L* combustion chamber had a 12.2-in long cylindrical section preceding nozzle convergence, which began abruptly. A short conical convergent section, with 30-degree-half-angle, was tangent to a circular arc throat section with a radius ratio of 2.00; the 5.70-in diameter throat was 15.7-in from the injector. Downstream of the throat, the throat circular arc was tangent to a 15-degree-half-angle expansion cone. The chamber contraction ratio and nozzle expansion ratio were 2.00 and 1.85, respectively. The nominal injector, designated LD-2, was flat-faced and had 112 like-doublet injection elements for each propellant. The elements were positioned geometrically to link each fuel doublet with an oxidizer doublet to form a like-doublet-pair. Among several like-doublet-pair injectors described in Ref. 10, only the selected LD-2 injector did not produce aligned fuel and oxidizer spray fans. As a result, propellant mixing efficiency - determined by cold-flow experiments - was substantially lower for the LD-2 injector than for the others; this was the reason for its selection as for the nominal checkout case. Nominal operating conditions were 100 psia chamber pressure and 5.2 mixture ratio.

VERIFICATION CASES

Also detailed in Ref. 10 are a large number of design and operating condition variations from the foregoing nominal checkout case. The validity of DER computer program performance predictions was evaluated

by comparing calculated efficiencies with the experimental results for several selected combinations of variables. Variations tested included injector design (aligned and non-aligned spray fans, enlarged orifices), chamber L* and contraction ratio, chamber pressure level and injection mixture ratio.

Integration of the TDK computer program into DER was accomplished very near the end of the contract period. As a result, most of the verification analysis was performed with a version of DER which terminated with STC generation of the TDK start-line. Most performance comparisons were limited, therefore, to c*-efficiency; these are discussed next, separately from specific impulse.

c* Efficiency Evaluations

Before proceeding with variation of design and operating conditions, two empirical adjustments were made to force the DER prediction of η_{c*} for the nominal checkout case to agree with its experimental value. The first of these was to position the STC initial-plane such that the value of E_m, Rupe's mixing efficiency factor, calculated by LISP matched the cold-flow experimental value reported in Ref. 10. Computed variation of E_m with z_o is shown in Fig. 8; from which z_o = 1.70-in was selected.

The second empirical adjustment concerned the LISP prediction of mean propellant drop sizes at the STC initial-plane. For like-doublet and like-doublet-pair elements, experimental c*-efficiencies were correlated analytically in Ref. 10 by

$$\eta_{c*} = \eta_{c*,\ mix}\ \eta_{evap} \tag{30}$$

where $\eta_{c*,\ mix}$ is a predicted c*-efficiency based on cold-flow measurement of spray mass and mixture ratio distribution, assuming complete evaporation and no further mixing, and η_{evap} is a calculated spray evaporation efficiency, derived from a one-dimensional combustion model which assumes complete mixing. η_{evap} depends strongly upon initial-

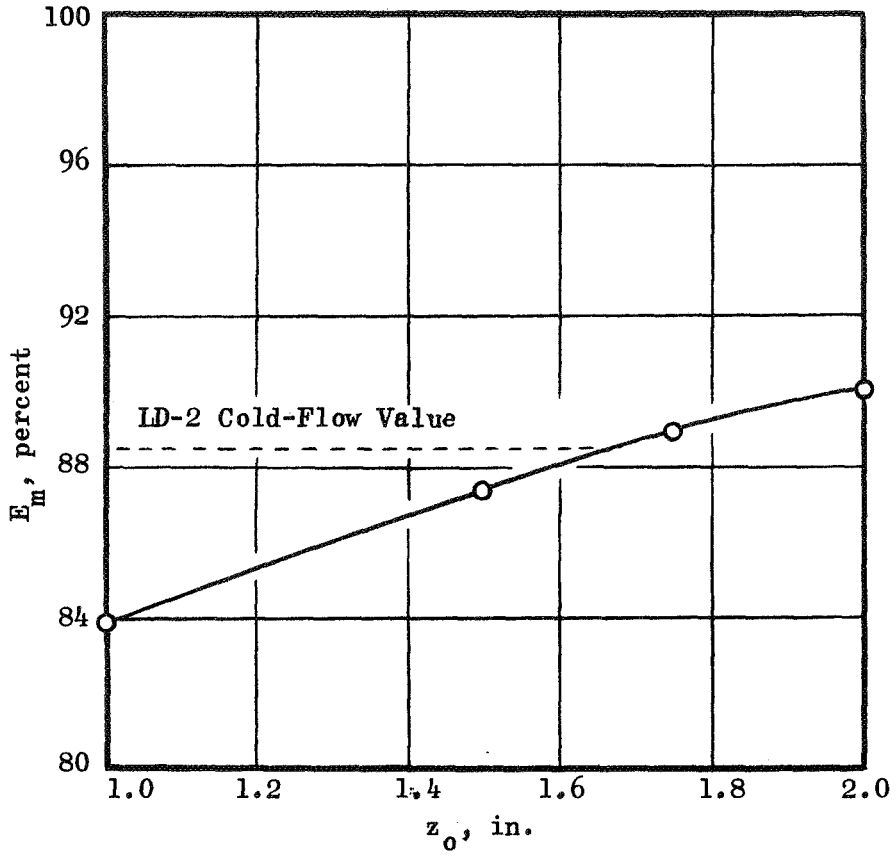

Figure 8. Calculated Variation of Mixing Efficiency vs LISP Collection Plane Position for LD-2 Like Doublet Injector

plane drop sizes. Correlation was achieved in Ref. 10 by using mean fuel drop diameters given by

$$D_{30} = \left\{ 2.64 \sqrt{\frac{V_j}{D_j}} + 0.97 \left[\frac{\left(\frac{\mu\sigma}{\rho}\right)_{\text{heptane}} \rho_g}{\left(\frac{\mu\sigma}{\rho}\right)_{\text{fuel}} \rho_{\text{air}}} \right]^{1/4} |V_g - V_j| \right\}^{-1}, \qquad (31)$$

assuming that the oxidizer (which is more volatile than the fuel) has the same mean drop size as the fuel, and empirically selecting a value for V_g such that predicted η_{c*} for a particular case was forced to agree with its corresponding experimental value. That value of V_g (320 ft/sec for $\varepsilon_c = 2$) was thereafter assumed to be a function (inverse variation) only of contraction ratio.

Equation 31 was used for both propellants, with the appropriate $(\mu\sigma/\rho)$ ratio, in the DER version of the LISP computer program. As might be expected, the mean oxidizer droplet diameters were not calculated to be identical to the fuel droplet sizes, as assumed in Ref. 10, but for most conditions were significantly smaller. DER predicted efficiencies using $V_g = 320$ ft/sec were thus substantially higher than the experimental values. Therefore, V_g was again empirically adjusted for the checkout case until agreement with the experimental η_{c*} was achieved. The derived value (190 ft/sec for $\varepsilon_c = 2$) was then used to predict η_{c*} for a series of other cases.

Results of these calculations are given in Table 1 and shown graphically in Fig. 9. Design data for the three like-doublet pair injectors considered are listed in Table 2. The predicted values of c*-efficiency were seen to agree quite well with the corresponding experimental values except for the one case in which the chamber contraction ratio was doubled. In that case, too coarse oxidizer atomization, resulting from a small value of $|V_g - V_j|$ in Eq. 31, produced unrealistically low oxidizer evaporation efficiency.

The combustion analysis of Ref. 10 was reviewed and compared with STC analysis to determine whether some difference other than the treatment

TABLE 1

VERIFICATION TEST CASE RESULTS

FLOX (80% F_2)/LPG (55% CH_4-45% C_2H_6)

Injector	Pc, psia	Mixture Ratio	L* in.	Contr. Ratio	η Evap. Calc.	η_{c*}, Mix		η_{c*}		$\Delta\eta_{c*}$
						Cold Flow	Calc.	Exptl.	Calc.	
LD-2	100	3.99	30	2.0	97.25	98.3	99.56	96.2	96.88	+ 0.68
↓	↓	5.19	↓	↓	97.24	95.6	96.26	93.3	93.27	- 0.03
↓	↓	6.41	↓	↓	97.01	95.7	95.33	92.9	92.19	- 0.71
LD-3	100	5.19	15	2.0	91.02	98.7	98.82	89.8	89.43	- 0.37
↓	↓	↓	30	↓	97.84	↓	↓	96.3	96.54	+ 0.24
↓	↓	↓	60	↓	99.72	↓	↓	98.1	98.51	+ 0.41
↓	50	↓	30	↓	97.67	98.2	98.59	95.2	96.06	+ 0.86
↓	200	↓	↓	4.0	84.59	98.7	99.18	93.1	83.57	- 9.53
LD-3M	100	5.24	15	2.0	91.97	98.4	98.32	88.9	89.23	+ 0.33
↓	↓	↓	30	↓	97.83	↓	↓	95.4	95.83	+ 0.43

TABLE 2

SUMMARY OF LIKE-DOUBLET INJECTOR SPECIFICATIONS (Ref. 10)

Injector Identification Number	Orifice Diameter		Nominal Injector ΔP (psi) at Design Conditions		d_{ox}/d_f	Fan Spacing, inch	Fan Inclination Angle, degrees	Intra-Element Spacing, inch
	Fuel, d_f, inch	Oxidizer, d_{ox}, inch	Oxidizer	Fuel				
LD-2	0.0200	0.0292	290	100	1.46	0.275	0	0.20
LD-3	↓	0.0360	85	↓	1.80	0.00	25	0.25
LD-3-M	0.0260	0.0469	30	30	↓	↓	↓	↓

Notes:

1. Like-doublet element is pair of fuel and oxidizer doublets.

2. All injectors contain six rings of elements. For each injector, the outer ring of elements are canted so that the resultant propellant spray is directed 15 degrees toward the axial centerline of the injector. Resultant propellant spray direction for the remaining elements is parallel to the chamber axis.

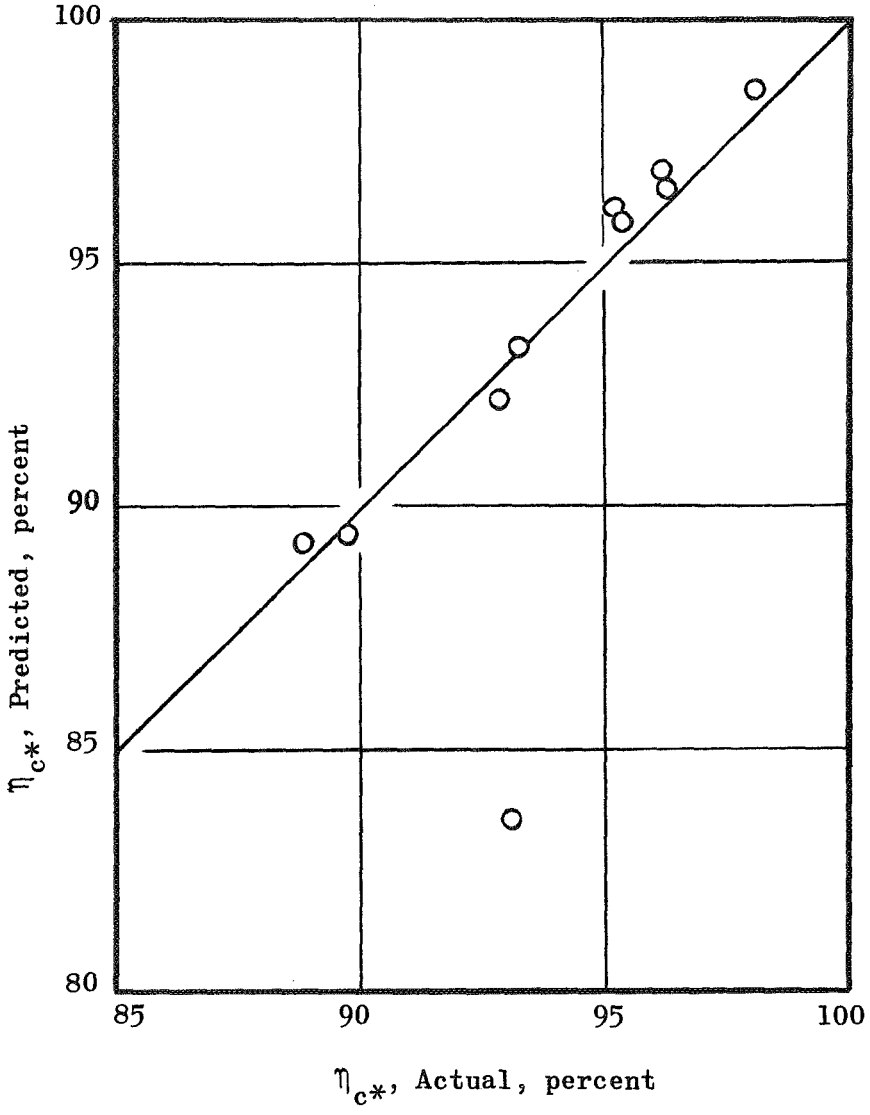

Figure 9. Comparison of Predicted and Actual C* Efficiencies for Verification Test Cases of Table 1

of oxidizer mean dropsize might account for the large disparity in derived values of V_g. It was concluded that there may be minor computational differences, both in the values of evaporation coefficients and in the treatment of droplet drag and evaporation, but that the major difference was in the methods used for distributing a propellant's flow rate into a number of droplet size groups. In Ref. 10, ten size groups with equal flow rate were formed and group diameters distributed according to empirical data from "cold-flow" like-doublet injection of molten wax (Ref. 7). In the foregoing DER analysis, spray flow rates had been distributed according to the Nukiyama-Tanasawa distribution function among six, equally-spaced droplet size groups.

Applying the former spray mass distribution to DER's six spray size groups permitted a higher value of V_g to be used than before, but a value of V_g = 240 ft/sec derived by analyzing two $\epsilon_c = 2$ cases was still substantially below the 320 ft/sec level. Continued difficulty in correlating $\epsilon_c = 4$ data was expected, therefore. Rather than recalculating several of the cases in Table 1, however, expected efficiencies were estimated by comparing predicted case droplet sizes with those sizes which gave the Table 1 results. This approach strengthened confidence in the ability of STC to predict $\epsilon_c = 2$ results, but indicated that performance of the $\epsilon_c = 4$ case would still be underpredicted by about 4 or 5 percent.

The DER c*-efficiency prediction for the $\epsilon_c = 4$ case was finally forced to match the experimental value by altering Eq. 31 for drop size prediction, so that it is contraction ratio dependent. Simultaneously, the mean diameter calculated was changed from D_{30} to the mass median diameter $\bar{D}$, which is the mean size used in the empirical mass distribution expression. The relationship $\bar{D} = 1.524\ D_{30}$ was adopted directly from the wax cold-flow results. Denoting $\left[(\mu\sigma/\rho)_{prop}/\rho_g\right]^{1/4}$ as C_{pr} and noting that $V_g = 240$ is really $480/\epsilon_c$ for $\epsilon_c = 2$ gives:

$$\bar{D} = 1.524 \left\{ 2.64 \left(\frac{V_j}{D_j}\right)^{1/2} + \frac{0.215}{C_{pr}} f(\epsilon_c) \left| \frac{480}{\epsilon_c} - V_j \right| \right\}^{-1} \qquad (32)$$

where an empirical function $f(\varepsilon_c)$ has been arbitrarily placed in the second term on the right. To fit the $\varepsilon_c = 4$ case and to have $f(2) = 1$ required:

$$f(\varepsilon_c) = \frac{5(\varepsilon_c - 1)}{\varepsilon_c + 3} \tag{33}$$

The $\varepsilon_c = 4$ case was run with Eq. 32 and 33 programmed in LISP; the predicted $\eta_{c*} = 92.53\%$ compared favorably with the experimental $\eta_{c*} = 93.1\%$.

Specific Impulse

Complete DER model calculations were made for only one of the cases listed in Table 1. The conditions for this selected case were the LD-3 injector at 100 psia chamber pressure and 5.19 mixture ratio in a 15-in L*, 2.0 contraction ratio chamber.

The coordinates of dividing streamlines and selected left-running-characteristics calculated by TDK are plotted in Fig. 10.

This case had been processes through LISP and STC with an equivalent V_g of 250 ft/sec (rather than the preferred 240 ft/sec); as a result, drop sizes were slightly small and the STC calculated η_{c*} was 90.71 percent, about 0.9 percent higher than the experimental value of 89.8 percent.

The TDK program block gives printed-out solutions for c*, I_s and C_F. The TDK prediction of c* efficiency was 2.2 percent higher than the experimental value. The TDK prediction of vacuum specific impulse was $I_s = 276.04$ lb_f-sec/lb_m compared with an experimental value, corrected to vacuum conditions of 269.5 lb_f-sec/lb_m; this difference is 2.4 percent of the experimental value.

In evaluating these results, it must be recognized that it is difficult to draw general conclusions from one test. The following discussion, therefore, must be regarded as tentative and somewhat speculative.

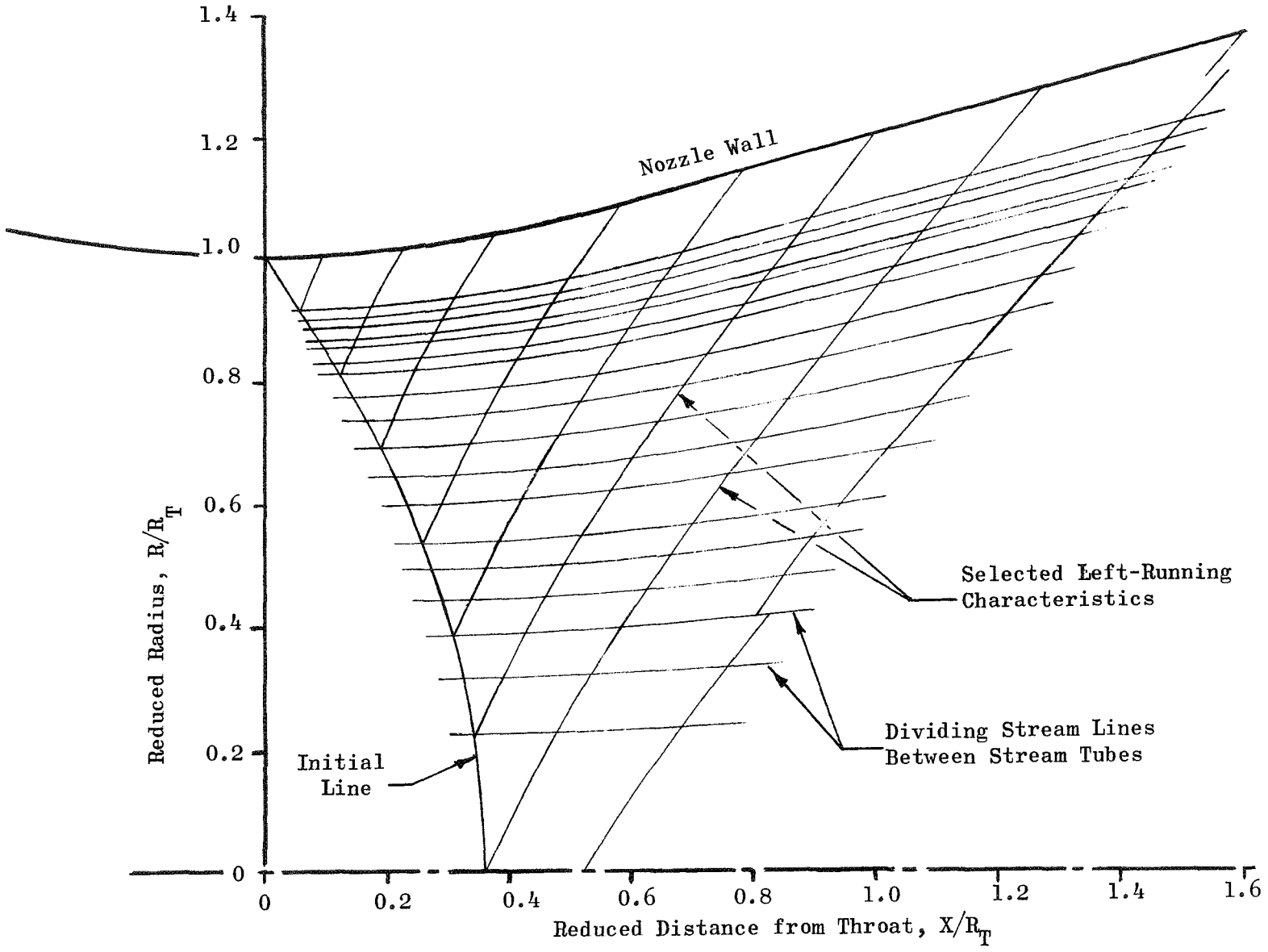

Figure 10. Selected Data from TDK Solution, 19 Stream Tubes of FLOX/LPG Combustion Gases in an $R_R = 2.0$, $\epsilon_e = 1.85$ Nozzle

This would be equally true even if the predicted performance figures had matched the experimental values precisely.

The vacuum thrust values in Ref. 10 had been corrected by 1.0 percent for combustor and nozzle heat transfer losses. By examination of calculated boundary layer losses for other combustors and conditions, it was inferred that the loss for this case should be about one percent. The implication is that both the predicted and experimental specific impulses should be lowered by about the same amount in accounting for boundary layer losses, i.e., essentially none of the 2.4 percent deviation can be attributed to boundary layer losses.

Possibly a strong contributor to the deviations in both c* and I_s is the discontinuity at the TDK initial-line which is a result of changing there from STC's frozen, isentropic local expansion (from the equilibrium stagnation temperature corresponding to the local gas mixture ratio) to a true equilibrium solution at the initial line. For the current verification case, the magnitude of the discontinuity was quite significant: the equilibrium static temperatures and molecular weights at the initial line were about 11 percent and 3 percent higher, respectively, than the corresponding STC computed values. With the initial line values of pressure and stream tube areas and gas velocities assumed to be invariant across the initial line, these combine to produce discontinuous drops of about 8 percent in stream tube gas densities and gas flowrates. This is substantially larger than the modest discontinuities that were anticipated and were expected to have only slight effects on prediction accuracy. Considering the equilibrium values to be the correct ones, the implication is that the pressure level for the entire STC analysis, including the TDK initial-line, is too low. This will not only affect the values of the initial line integrals upon which TDK's computation of c* and thrust are based but may change the spray vaporization efficiency as well. Interestingly, these effects should cause the c* and I_s predictions to deviate by comparable magnitudes, as was observed.

(Correction of the TDK initial-line discontinuity ideally would involve using local equilibrium solutions throughout the STC program analysis. That would require a moderate amount of reprogramming and checkout but, more importantly, STC computation times would be drastically increased. Before going to that extreme, some alternative approaches should be examined. One such alternative is simply replacing the frozen values of $\gamma(c_i)$ in the combustion gas properties table with the shifting values. A cursory examination of the current case suggests that the temperature discontinuity might be reduced to 2 to 3 percent by this approach.)

CONCLUSIONS

1. A series of existing computer programs has been successfully modified and combined into a single operable computer program that is capable of predicting liquid rocket engine performance.
2. The developed performance model was found to be capable of predicting engine c*-efficiencies within approximately ± 1 percent as verified by comparison with a limited amount of like-doublet-pair injected FLOX/LPG propellant hot-firing data. Achieving comparable accuracy for other propellants or injectors may depend upon adjustment of empirical parameters to force agreement with one or more experimental data points.
3. The validity of the model's predictions of specific impulse was not as well verified as were its c*-efficiency predictions. Some further model refinements will be required to achieve ± 1 percent accuracy on I_s.
4. Operation of the model, and the validity of its predictions, depended strongly upon valid cold-flow spray mass distribution and drop size correlations for the particular type of injection element under study.

RECOMMENDATIONS

The following work is recommended to extend the verified applicability of the developed performance analysis model to wider ranges of designs, propellants and operating conditions:

1. Perform additional verification analysis of the model's capability for predicting specific impulse.
2. Reduce or eliminate the gas-phase properties discontinuity at the STC-TDK interface.
   a. Evaluate use of shifting γ in STC computations and/or
   b. Use full shifting equilibrium throughout STC.
3. Refine the planar-to-curved-isobar transition, retaining precise area continuity to the immediate neighborhood of the throat.
4. Supplement the transonic flow pressure distribution near the throat with a subsonic model for conical or tapered combustion chambers.
5. Improve the treatment of spray droplet vaporization, accounting for droplet heating and combustion at supercritical pressures.
6. Extend the program's capabilities to gas/liquid propellants.
7. Calculate and punch out data needed for subsequent analysis with the TBL (Turbulent Boundary Layer) computer program.
8. Include 3D-COMBUST analysis of the rapid combustion zone.
9. Simplify computer program input.
10. Improve computational efficiency to reduce execution times.
11. Assemble a library of available injector design correlations.

NOMENCLATURE

A	=	area
a	=	local sound speed
$a, b, C_1 \text{---} C_6$	=	empirical spray coefficients, Eq. 2
C_D	=	drag coefficient
$C_{k'}$	=	approximate evaporation coefficient
C_{ND}	=	nozzle discharge coefficient
C_{pr}	=	coefficient involving propellant properties, Eq. 32
c	=	mixture ratio
c^*	=	characteristic exhaust velocity
C_F	=	thrust coefficient
c_p	=	specific heat at constant pressure
D	=	droplet or liquid jet diameter
$\bar{D}$	=	mass median droplet diameter
D_{30}	=	volume-number mean droplet diameter
E_m	=	Rupe mixing efficiency factor (Ref. 6)
F	=	drag force
$f(\varepsilon_c)$	=	function of contraction ratio, Eq. 32 and 33
g_c	=	gravitational coefficient
I_s	=	specific impulse
ΔH_v	=	heat of vaporization
k_g	=	thermal conductivity
k_s'	=	droplet evaporation coefficient
M_w	=	molecular weight
m	=	droplet mass or spray size group mass
$\dot{m}$	=	rate of change of mass
N	=	droplet concentration (no/volume)
$\dot{N}$	=	number flowrate of droplets
N_{EL}	=	number of injection elements
Nu	=	Nusselt number
n_t	=	number of stream tubes
p	=	pressure

p^*	=	pressure corresponding to sonic flow
Re	=	Reynolds number
R_u	=	universal gas constant
R_R	=	nozzle throat radius ratio (curvature/opening)
R_T	=	nozzle throat radius
r	=	radial coordinate
s	=	stream tube path length
T	=	temperature
u, V	=	velocity
V_g	=	empirical parameter in atomization equation, Eq. 31
W	=	propellant mass flux at a spatial mesh point
w	=	propellant mass flux contribution from an injection element to a mesh point
w_{001}	=	$w(x,y,z)$ for $x=y=0$, $z=1$
$\dot{W}$, w	=	total and local (or stream tube) flowrates
x,y,z	=	rectangular coordinates (referenced to an injection element)
z	=	axial coordinate
z_o	=	initial plane for beginning spray combustion analysis

GREEK LETTERS

α	=	nozzle wall angle (from chamber axis)
γ	=	ratio of specific heats or adiabatic expansion coefficient
ϵ_c	=	chamber contraction ratio
ϵ_e	=	nozzle expansion ratio
ϵ_{A_T}	=	decimal tolerance, convergence on throat area
η	=	efficiency factor
θ	=	angular coordinate
μ	=	viscosity
ρ	=	density
σ	=	surface tension

SUPERSCRIPTS

$(\bar{})$	=	average value or concerned with one-dimensional solution
n	=	concerned with the n^{th} droplet size group

SUBSCRIPTS

c	=	chamber
d	=	droplet
e	=	expansion section
F	=	fuel
g	=	combustion gas
i	=	concerned with i^{th} injection element, mesh point radial index or stream tube
j	=	concerned with j^{th} propellant
ℓ	=	liquid
O	=	oxidizer
o	=	initial or stagnation value
s	=	surface or stream tube path
v	=	vapor or vaporization

REFERENCES

1. Pieper, J. L., "ICRPG Liquid Propellant Thrust Chamber Performance Evaluation Manual," CPIA Publ. No. 178, Chemical Propulsion Information Agency, Silver Spring, Md., September 1968.

2. Hines, W. S., Combs, L. P., Ford, W. M., and VanWyk, R., "Development of Injector Chamber Compatibility Analysis," Final Report, AFRPL-TR-70-12, Rocketdyne, a Division of North American Rockwell Corp., Canoga Park, Calif., March 1970.

3. Combs, L. P. and Chadwick, W. D., "Liquid Rocket Performance Computer Model with Distributed Energy Release, Computer Program Documentation," Rocketdyne, a Division of North American Rockwell Corporation, Canoga Park, Calif., September 1970.

4. Sutton, R. D., Hines, W. S., and Combs, L. P., "Comprehensive Analysis of Liquid Rocket Combustion," AIAA Paper No. 70-622, June 1970.

5. Kliegel, J. R., et al, "ICRPG Two-Dimensional Kinetic Reference Program," Dynamic Science, a Division of Marshall Industries, Irvine, Calif., July 1968.

6. Rupe, J. H. and Jaivin, G. H., "The Effects of Injection Mass Flux Distributions and Resonant Combustion on Local Heat Transfer in a Liquid Propellant Rocket Engine," Prog. Rpt. 32-648, Jet Propulsion Laboratory, Pasadena, Calif., October 1964.

7. Dickerson, R. A., Tate, K. and Barsic, N., "Correlation of Spray Injector Parameters with Rocket Engine Performance," Final Report, AFRPL-TR-68-147, Rocketdyne, a Division of North American Rockwell Corporation, Canoga Park, Calif., June 1968

8. Nickerson, G. R., "Instructions for Replacing the Transonic Analysis of the TDK Computer Program," Dynamic Science Letter Report, received April 1970.

9. Kliegel, J. R. and Levine, J. N., "Transonic Flow in Small Throat Radius of Curvature Nozzles," AIAA Journal, Vol. 7, No. 7, July 1969.

10. Falk, A. Y., Clapp, S. D. and Nagai, C. K., "Space Storable Propellant Performance Study," Final Report, NASA CR-72487, Rocketdyne, a Division of North American Rockwell Corporation, Canoga Park, Calif., November 1968.

APPENDIX A

Distribution List for Final Report NASA CR-
"Liquid Rocket Performance Computer Model
with Distributed Energy Release"
NAS7-746
Rocketdyne Division
North American Rockwell Corporation

		COPIES
National Aeronautics and Space Administration Washington, D. C. 20546		
Attention:	Contracting Officer	1
	Patent Office	1
National Aeronautics and Space Administration Lewis Research Center 21000 Brookpark Road Cleveland, Ohio 44135		
Attention:	Office of Technical Information	1
	Dr. R. J. Priem	1
	Larry Gordon	1
	E. W. Conrad	1
	Sanford Gordon	1
National Aeronautics and Space Administration Manned Spacecraft Center Houston, Texas 77001		
Attention:	Office of Technical Information	1
	J. G. Thibodaux, Jr.	1
	Ronald C. Kahl	1
National Aeronautics and Space Administration Marshall Space Flight Center Huntsville, Alabama 35812		
Attention:	Technical Library	1
	Dale Burrows, S&E - ASTN - PJ, Bldg. 4666	1
National Aeronautics and Space Administration Ames Research Center Moffatt Field, California 94035		
Attention:	Contracting Officer, R&D Contracts Section (ASCR)	1
	Mission Analysis Division	1
	Alberta Alksne, N-203-9	1

	COPIES
Jet Propulsion Laboratory 4800 Oak Grove Drive Pasadena, California 91103	
Attention: Jack H. Rupe	2
Henry Burlage, Jr., Propulsion Div. 38	2
Walter B. Powell	1
National Aeronautics and Space Administration Washington, D.C. 20546	
Attention: Chief, Liquid Propulsion Technology RPL Office of Advanced Research and Technology	3
Director, Technology Utilization Division Office of Technology Utilization	1
Director, Launch Vehicles and Propulsion, SV Office of Space Science and Applications	1
Director, advanced Manned Missions, MT Office of Manned Space Flight	1
National Aeronautics and Space Administration P.O. Box 33 College Park, Maryland 20740	
Attention: Scientific and Technical Information Facility	25
Langley Research Center Langley Station Hampton, Virginia 23365	
Attention: Ed Cortwright, Director	2
Lewis Research Center 21000 Brookpark Road Cleveland, Ohio 44135	
Attention: Dr. Abe Silverstein, Director	2
National Aeronautics and Space Administration John F. Kennedy Space Center Cocoa Beach, Florida 32931	
Attention: Dr. Kurt H. Debus	2
Aeronautical Systems Division Air Force Systems Command Wright-Patterson Air Force Base Dayton, Ohio 45433	
Attention: D. L. Schmidt, Code ASRCNC-2	1
Arnold Engineering Development Center Arnold Air Force Station Tullahoma, Tennessee 37388	
Attention: Dr. H. K. Doetsch	1

	COPIES
Bureau of Naval Weapons Department of the Navy Washington, D. C. 20546 Attention: J. Kay, RTMS-41	1
Defense Documentation Center Headquarters Cameron Station, Building 5 5010 Duke Street Alexandria, Virginia 22314 Attention: TISIA	1
Picatinny Arsenal Dover, New Jersey 07801 Attention: I. Forsten, Chief, Liquid Propulsion Laboratory	1
Air Force Rocket Propulsion Laboratory Research and Technology Division Air Force Systems Command Edwards, California 93523 Attention: RPRPD/Mr. H. Main RPRRC/Wayne C. Pritz Thomas J. Fanciullo	1 1 1
U. S. Army Missile Command Redstone Arsenal, Alabama 35809 Attention: Mr. Walter Wharton	1
U. S. Bureau of Mines 4800 Forbes Avenue Pittsburgh, Pennsylvania 15213 Attention: Mr. Henry Perlee	1
U. S. Naval Ordnance Test Station China Lake, California 93557 Attention: D. Couch	1
Air Force Office of Scientific Research 1400 Wilson Boulevard Arlington, Virginia 22209 Attention: B. T. Wolfson	1
Chemical Propulsion Information Agency Applied Physics Laboratory 8621 Georgia Avenue Silver Spring, Maryland 20910 Attention: Tom Reedy	1

	COPIES
Aerojet Liquid Rocket Company Sacramento, California Attention: Jack Ito	1
D. L. Kors	1
Aerojet-General Corporation P.O. Box 296 Azusa, California 91703 Attention: W. L. Rogers	1
Space Division Aerojet-General Corporation 9200 East Flair Drive El Monte, California 91734 Attention: S. Machlawski	1
Aerospace Corporation 2400 East El Segundo Boulevard P.O. Box 95085 Los Angeles, California 90045 Attention: O. W. Dykema	1
W. B. Roessler	1
Atlantic Research Corporation Edsall Road and Shirley Highway Alexandria, Virginia 22314 Attention: Librarian	1
Bell Aerosystems Company P.O. Box 1 Buffalo, New York 14240 Attention: W. M. Smith	1
Boeing Company P.O. Box 3707 Seattle, Washington 98124 Attention: J. D. Alexander	
Wright Aeronautical Division Curtiss-Wright Corporation Woodridge, New Jersey 07075 Attention: G. Kelley	1
Dynamic Science Division Marshall Industries Irvine, California Attention: G. Nickerson	1
T. Kosvic	1

	COPIES
Research Center Fairchild Hiller Corporation Germantown, Maryland Attention: Ralph Hall	1
Missile and Space Systems Center General Electric Company Valley Forge Space Technology Center P.O. Box 8555 Philadelphia, Pennsylvania Attention: F. Mezger F. E. Schultz	1 1
Gurmman Aircraft Engineering Corporation Bethpage, Long Island New York 11714 Attention: Joseph Gavin	1
Honeywell, Inc. Aerospace Division 2600 Ridgeway Road Minneapolis, Minnesota Attention: Mr. Gordon Harms	1
Hughes Aircraft Company Aerospace Group Centinella and Teale Streets Culver City, California 90230 Attention: E. H. Meier, V.P. and Division Manager, Research and Development Division	1
Arthur D. Little, Inc. 20 Acorn Park Cambridge, Massachusetts 02140 Attention: Library	1
Lockheed Propulsion Company P.O. Box 111 Redlands, California 92374 Attention: H. L. Thackwell	1
The Marquardt Corporation 16555 Saticoy Street Van Nuys, California 91409 Attention: Howard McFarland	1

		COPIES
Denver Division Martin Marietta Corporation P.O. Box 179 Denver, Colorado 80201		
Attention:	Dr. Morganthaler	1
	A. J. Kullas	1
	William Scott	1
Astropower Laboratory Newport Beach, California 92663		
Attention:	Dr. George Moc	1
Missile and Space Systems Division McDonnell-Douglas Aircraft Company 3000 Ocean Park Boulevard Santa Monica, California 90406		
Attention:	Mr. R. W. Hallet, Chief Engineer Advanced Space Technology	1
Space and Information Systems Division North American Rockwell Corporation 12214 Lakewood Boulevard Downey, California 90241		
Attention:	Library	1
Northrop Space Laboratories 3401 West Broadway Hawthorne, California 90250		
Attention:	Dr. William Howard	1
Florida Research and Development Center Pratt and Whitney Aircraft Corporation West Palm Beach, Florida		
Attention:	Robert Carroll	1
	B. D. Powell	1
Stanford Research Institute 333 Ravenswood Avenue Menlo Park, California 94025		
Attention:	Dr. Gerald Marxman	1
TRW Systems Group TRW, Incorporated One Space Park Redondo Beach, California 90278		
Attention:	S. S. Cherry	1

	COPIES
Reaction Motors Division Thiokol Chemical Corporation Denville, New Jersey 07832 Attention: Dwight S. Smith	1
Research Laboratories 400 Main Street East Hartford, Connecticut 06108 Attention: Erle Martin	1
United Technology Center 587 Methilda Avenue P.O. Box 358 Sunnyvale, California 94088 Attention: Dr. David Altman	1
University of Michigan Aerospace Engineering Ann Arbor, Michigan 48104 Attention: J. A. Nicholls	1
University of California Department of Chemical Engineering 6161 Etcheverry Hall Berkeley, California 94720 Attention: A. K. Oppenhiem R. Sawyer	1 1
Purdue University School of Mechanical Engineering Lafayette, Indiana 47907 Attention: J. M. Osborn	1
Sacramento State College Engineering Division 60000 J. Street Sacramento, California 95819 Attention: E. H. Reardon	1
Illinois Institute of Technology Room 200 M. H. 3300 South Federal Street Chicago, Illinois 60616 Attention: T. P. Torda	1

COPIES

Polytechnic Institute of Brooklyn
Graduate Center
Route 110
Farmingdale, New York
Attention: V. D. Agusta — 1

Georgia Institute of Technology
Atlanta, Georgia 30332
Attention: B. T. Zinn — 1

University of Denver
Research Institute
Denver, Colorado
Attention: W. H. McLain — 1

New York University
Department of Chemical Engineering
University Heights
New York 53, New York
Attention: Leonard Dauerman — 1

The Johns Hopkins University
Applied Physics Laboratory
8621 Georgia Avenue
Silver Springs, Maryland 20910
Attention: W. G. Berl

Princeton University
Forrestal Campus
Guggenheim Laboratories
Princeton, New Jersey 08540
Attention: I. Glassman — 1

The University of Sheffield
Department of Fuel Technology
St. George's Square
Sheffield 1. Yorks, England
Attention: Mr. J. Swithenbank — 1

Motorear Enstitusu
Professor Zubeyir Demirgue
Director of Engine Institute
Istanbul - Gumussuyu — 1

Instituto Nacional
De Tecnica Aerospacial
Carlos Sanchez-Tarifa
Serrano 43
Madrid, Spain — 1